NASA TECHNICAL NOTE

NASA TN D-2651

BRAYTON CYCLE MAGNETOHYDRODYNAMIC POWER GENERATION WITH NONEQUILIBRIUM CONDUCTIVITY

by John E. Heighway and Lester D. Nichols

Lewis Research Center
Cleveland, Ohio

NATIONAL AERONAUTICS AND SPACE ADMINISTRATION • WASHINGTON, D. C. • FEBRUARY 1965

BRAYTON CYCLE MAGNETOHYDRODYNAMIC POWER GENERATION

WITH NONEQUILIBRIUM CONDUCTIVITY

By John E. Heighway and Lester D. Nichols

Lewis Research Center
Cleveland, Ohio

NATIONAL AERONAUTICS AND SPACE ADMINISTRATION

BRAYTON CYCLE MAGNETOHYDRODYNAMIC POWER GENERATION

WITH NONEQUILIBRIUM CONDUCTIVITY

by John E. Heighway and Lester D. Nichols

Lewis Research Center

SUMMARY

Power densities of magnetohydrodynamic generators operating in a Brayton cycle with nonequilibrium conductivity are computed. Helium, neon, argon, and xenon with cesium seed are considered as working fluids in a constant-area, constant-voltage segmented generator operating in the Faraday mode. The generator performance is specified by optimizing the cycle efficiency with respect to load voltage and by optimizing output power density with respect to seed fraction and operating pressure. The power density is determined as a function of Mach number and magnetic field strength. Argon exhibits the highest power density in the supersonic regime and neon the highest in the subsonic regime for the particular generator and cycle considered.

INTRODUCTION

Techniques of magnetohydrodynamic power generation are being studied with increasing interest for use in space as the development of high temperature materials and high field strength magnets progresses. Devices using these techniques are to take the place of the turbogenerator in a conventional power generation cycle. Several schemes have been proposed that combine Rankine, Brayton, Ericsson, or hybrid cycles with liquids, vapors, and mixtures of these two as proposed working fluids (refs. 1 to 4). Those devices that have a vapor in the generator are especially adaptable to the space power requirements, but the vapor has low electrical conductivity at temperatures compatible with materials. As a result, several schemes for increasing the electrical conductivity at low gas temperatures have been proposed (refs. 3, 5, 6, and 7).

One such scheme may be used in a Brayton cycle where the working fluid is an alkali metal vapor seeded in a noble gas. This scheme utilizes the induced electric field of the plasma to increase the electron temperature (ref. 8). This effect, sometimes called the Kerrebrock effect, has been studied extensively (refs. 9 to 11). Each of these studies considers a particular noble gas and seed for which high conductivity was attained. In these studies, however, no attempt has been made to compare the behavior of different working fluids for a specified generator operating under conditions appropriate for space application.
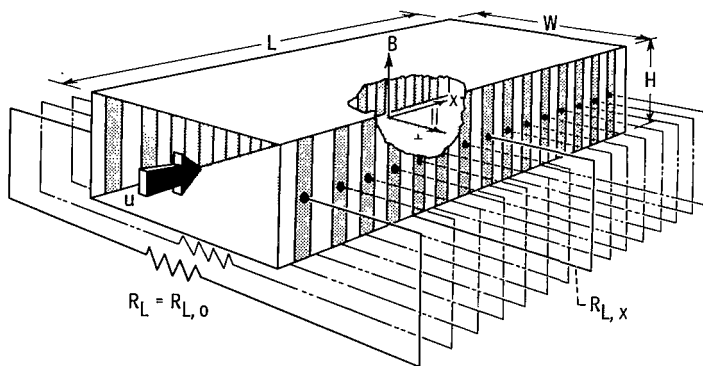
Figure 1. - Schematic representation of Faraday segmented generator.

In this study a constant-area linear duct with segmented electrodes operating as a Faraday generator (ref. 12) is studied. The magnetic field is constant and unaffected by the fluid. The current through each pair of electrodes is adjusted so that the generated voltage is constant. The working fluid is a noble gas seeded with cesium, and the effects of viscosity and heat conduction are neglected. Generators of this configuration have been studied previously (refs. 13 to 16). The studies of Neuringer and of Coe and Eisen consider both constant and equilibrium conductivity dependent on local temperature, but neither considers nonequilibrium conductivity. Recently, McNab and Cooper (ref. 17) presented solutions for this generator including the effect of nonequilibrium conductivity for a helium cesium plasma. Their analysis is not for a constant voltage but for a voltage proportional to the local velocity. They included the effect of friction and heat transfer and discovered that the electrical interactions are the dominant flow control mechanisms. Since they showed that friction and heat transfer can be neglected, a study of a generator with constant voltage and nonequilibrium conductivity will be made. The comparison between different seeded noble gas working fluids will be examined for the optimum conditions to be obtained.

ANALYSIS OF GENERATOR CHARACTERISTICS

A linear magnetohydrodynamic generator is analyzed using the one-dimensional fluid flow equations. The fluid is considered to be a perfect gas, and the effects of heat conduction and viscosity are neglected. The electrical conductivity is to be calculated using the concept of magnetically induced ionization (refs. 8 to 11), which implies an elevated electron temperature. This elevated temperature is the result of an energy balance between the energy added to the electrons by the induced electric field and the energy lost by the electrons upon collision with the other particles. This energy balance is performed in detail in the section DETERMINATION OF NONEQUILIBRIUM CONDUCTIVITY.

Development of Magnetohydrodynamic Equations

The continuity, momentum, energy, and state equations for the generator shown in figure 1 are the following (ref. 18):

$$\frac{d}{dx}(\rho u) = 0 \tag{1}$$

$$\rho u \frac{du}{dx} + \frac{dp}{dx} + jB = 0 \tag{2}$$

2

$$\rho u \frac{dh}{dx} + \rho u^2 \frac{du}{dx} - jE_\perp = 0 \qquad (3)$$

$$h = \frac{\gamma}{\gamma - 1} \frac{p}{\rho} \qquad (4)$$

where $E_\perp$ is the transverse component of electric field. (All symbols are defined in appendix A.)

The restriction imposed by Maxwell's equation, curl $\vec{E} = -\partial B/\partial t$, for a constant magnetic field and a one-dimensional problem require that $E_\perp$ be a constant, equal to $-V/W$, throughout the channel. This constant can be expressed as some fraction of the entrance open-circuit field u_0B as

$$K = \frac{V}{u_0 BW}$$

where K will be called the load parameter.

The generator is assumed to be segmented, and the segments are assumed to be infinitely thin, so that no axial currents flow. The proper Ohm's Law is (ref. 11)

$$j = \sigma \left(uB - \frac{V}{W} \right) \qquad (5)$$

where σ includes Hall effects and ion slip, and $\vec{j}$ is parallel to $\vec{u} \times \vec{B}$. The restriction that K be a constant places a restriction on the load resistance R_L:

$$(A_e j)R_L = (A_e j)_0 R_{L,0} = \text{constant}$$

where the subscript zero denotes entrance values. If all electrodes are given the same area A_e, the current can be eliminated as follows:

$$\frac{R_{L,0}}{R_L} = \frac{j}{j_0} = \frac{\sigma \left(\dfrac{u}{u_0} - K \right)}{\sigma_0 (1 - K)} \qquad (6)$$

To solve the system of equations (1) to (4), the enthalpy h can be eliminated by using equation (4) and the momentum and energy equations. The resulting expression can be integrated to obtain the following relation between the pressure and velocity:

$$(\rho u^2 + p) - (\rho_0 u_0^2 + p_0) = \frac{BW}{V} \left[\left(\frac{\gamma}{\gamma - 1} up + \frac{\rho u^3}{2} \right) - \left(\frac{\gamma}{\gamma - 1} u_0 p_0 + \frac{\rho_0 u_0^3}{2} \right) \right] \qquad (7)$$

3

At this point, it is convenient to introduce the following nondimensional variables and parameters:

$$U \equiv \frac{u}{u_0} \qquad\qquad K_1 \equiv \frac{\gamma - 1}{\gamma} K$$

$$P \equiv \frac{p}{\rho_0 u_0^2} \qquad\qquad M_1 \equiv 1 - \frac{2}{\gamma + 1}\left(1 - \frac{1}{M_0^2}\right)$$

$$M_0^2 \equiv \frac{u_0^2 \rho_0}{\gamma p_0} \qquad\qquad \Upsilon^2 \equiv (1 - K_1)(M_1 - K_1)$$

Equation (7) may then be expressed as

$$\gamma P = U - \frac{\gamma + 1}{2}\left(U - K_1 - \frac{\Upsilon^2}{U - K_1}\right) \tag{8}$$

Equation (8) represents the relation between pressure and velocity. Since the duct is segmented with infinitely thin segments, the power developed in the generator can be obtained by integrating the product of voltage and current $VjH\,dx$ over the length of the generator:

$$\Pi = \int_0^L VjH\,dx = \rho_0 u_0^3 KWH\left[\left(1 + \frac{1}{\gamma M_0^2}\right) - (U + P)\right] \tag{9}$$

This power can be compared to the total enthalpy flux entering the generator:

$$\text{Total enthalpy flux} = \rho_0 u_0 WH\left(\frac{\gamma}{\gamma - 1}\frac{p_0}{\rho_0} + \frac{1}{2}u_0^2\right) \tag{10}$$

The ratio of these terms is called the conversion effectiveness η_{conv} and may be written as

$$\eta_{conv} = \frac{K_1(1 - U)}{(U - K_1)}\frac{(U - M_1)}{M_1} \tag{11}$$

The power output of a generator with a specified inlet condition can now be determined. In order to calculate the output power density, however, a relation between velocity and generator length must be determined. The two variables, dimensionless conductivity $\Sigma \equiv \sigma/\sigma_0$ and dimensionless interaction length ξ, defined by

$$\xi \equiv \frac{\sigma_0 B^2 x}{\rho_0 u_0}$$

4

are introduced. Equation (2) can then be written as

$$\frac{d}{d\xi}(U + P) + \Sigma(U - K) = 0 \tag{12}$$

which can be expressed as

$$\xi = \int_U^1 \frac{1 + \frac{\partial P}{\partial U}}{\Sigma(U)(U - K)} \, dU \tag{13}$$

Equation (13) provides a relation between U and the interaction length. An expression for $\partial P/\partial U$ can be obtained by differentiating equation (8):

$$\frac{\partial P}{\partial U} = \frac{1}{\gamma} - \frac{\gamma + 1}{2\gamma}\left[1 + \left(\frac{\Upsilon}{U - K_1}\right)^2\right] \tag{14}$$

so that equation (13) becomes

$$\xi = \frac{\gamma + 1}{2\gamma}\int_U^1 \frac{1 - \left(\frac{\Upsilon}{U - K_1}\right)^2}{\Sigma(U)(U - K)} \, dU \tag{15}$$

It is noticed that if the conductivity is constant $(\Sigma = 1)$, equation (15) can be integrated:

$$\xi_{const} = \frac{\gamma + 1}{2\gamma}\left\{\left[1 - \left(\frac{\Upsilon}{K}\right)^2\right]\ln\left(\frac{1 - K}{U - K}\right) + \left(\frac{\Upsilon}{K}\right)^2\ln\left(\frac{1 - K_1}{U - K_1}\right) - \left(\frac{\Upsilon}{K}\right)^2\frac{K}{\gamma}\left(\frac{1}{1 - K_1} - \frac{1}{U - K_1}\right)\right\} \tag{16}$$

which is in agreement with the results of other investigations (refs. 1, 16, and 19).

By using equation (15) for interaction length, it is possible to express the output power density as follows:

$$\mathscr{P} = \frac{\Pi}{WHL} = \sigma_0 u_0^2 B^2 \frac{K_1(\gamma + 1)(1 - U)(U - M_1)}{2(\gamma - 1)(U - K_1)\xi} \tag{17}$$

This is the power density for a constant-area generator. It is of interest to gage the effect of velocity variation as well as conductivity variation. The

5

power density at the entrance to the generator is

$$\mathscr{P}_0 = \sigma_0 u_0^2 B^2 K (1 - K) \tag{18}$$

The ratio of equation (17) to equation (18)

$$\frac{\mathscr{P}}{\mathscr{P}_0} = \frac{(\gamma + 1)(1 - U)(U - M_1)}{2\gamma \xi (U - K_1)(1 - K)} \tag{19}$$

will be used for comparison. This ratio will be calculated for the constant conductivity case, where ξ_{const} is given by equation (16), and for ξ as determined from equation (15) by use of the nonequilibrium conductivity.

The cycle thermodynamic efficiency may be conveniently expressed in terms of a generator (isentropic) efficiency. This efficiency, which is defined as the actual change in total enthalpy of the working fluid in the generator compared to the change in total enthalpy for an isentropic process between the same total pressure conditions, is derived in appendix B. The thermodynamic cycle efficiency for the Brayton cycle under conditions appropriate for space application is also calculated in appendix B. Certain limiting values for η_{conv}, however, can be obtained without specifying the conductivity.

<center>Limiting Case</center>

From equation (13) it can be seen that, as U approaches K, ξ will approach infinity; obviously, this is a limiting value for U. This situation represents the maximum interaction length and, consequently, the maximum amount of energy that can be taken from the fluid. In some cases, however, the interaction length cannot become indefinitely large. It is limited by the phenomenon called "choking", which can be characterized by the criterion that the local Mach number reaches 1. In the dimensionless symbols defined previously, this condition is equivalent to

$$U = \gamma P \tag{20}$$

This condition, when substituted into equation (8), leads to the following specification of U at choking:

$$U_{ch} = K_1 + \gamma \tag{21}$$

It is noticed that this is the value of the velocity for which the integrand in equation (15) is zero; that is, U_{ch} is the condition that makes $\partial \xi / \partial U = 0$.

Two different operation limits have been described: first, when $U = K$ and the duct is infinitely long, and second, when $U = U_{ch}$ and the duct is choked. For any generator operation the proper limiting value can be determined by considering the case where the duct is choked at infinity. Formally speaking, this occurs when $U_{ch} = K$. This condition can be substituted into equation (21) and the K for which this occurs (call it K_∞) can be determined
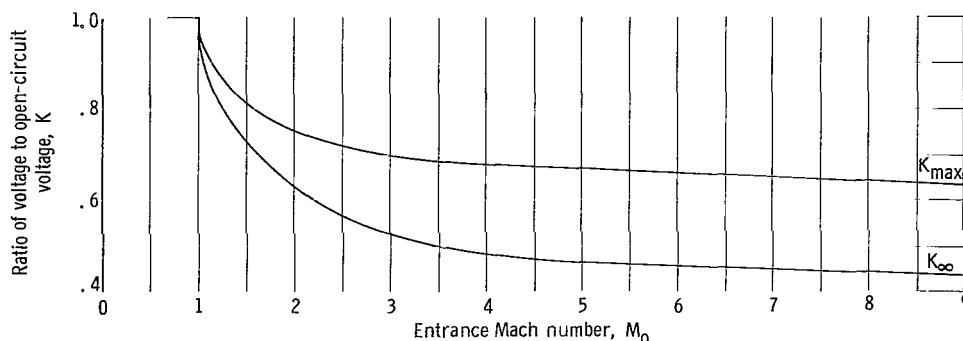
Figure 2. - Load parameters for maximum thermal efficiency and infinite choking length for initial compressor efficiency of 0.80.

from the following:

$$K_\infty = \frac{\gamma - 1}{\gamma} K_\infty + \Upsilon$$

which may be written as

$$K_\infty = \gamma \frac{\sqrt{\frac{(\gamma - 1)^2(1 - M_1)^2}{4} + M_1} - \frac{(\gamma - 1)(1 + M_1)}{2}}{1 - (\gamma - 1)^2} \tag{22}$$

The criterion for distinguishing between the two limiting case may therefore be stated as follows: For $K > K_\infty$, the duct will not choke and U will approach K, while for $K < K_\infty$, the duct will be choked and U will approach U_{ch}. The duct is infinitely long and choked for $K = K_\infty$. When $\gamma = 5/3$, K_∞ is as shown in figure 2. It is noted that for $M_0 < 1$ the duct will always choke, if sufficiently long, since K must be less than 1; whereas, as shown in equation (22) K_∞ must be greater than unity.

The quantity η_{conv} can be calculated from equation (11) and η_S from appendix B for a specified γ and Mach number as a function of K. Therefore, the thermal efficiency η_{th} can be calculated by means of equation (B11) for a specified compressor efficiency and regenerator effectiveness. In figure 3(a) (p. 8) this efficiency is plotted for $\gamma = 5/3$, $M_0 = 2.0$, and $\eta_{comp} = 0.8$ with regenerator effectiveness as a parameter. Two items should be noted: First, the efficiency has a maximum at some values of K, and second, this value of K is independent of η_r even though the efficiency varies with η_r (this is true for all supersonic Mach numbers). The value of K also depends on η_{comp}, but that dependency will not be investigated.

In figure 3(b) the efficiency is plotted again as a function of K with $\gamma = 5/3$ and $\eta_{comp} = 0.8$, but with $\eta_r = 0$ and Mach number as the parameter. It can be seen that the K for the optimum efficiency does depend on the Mach
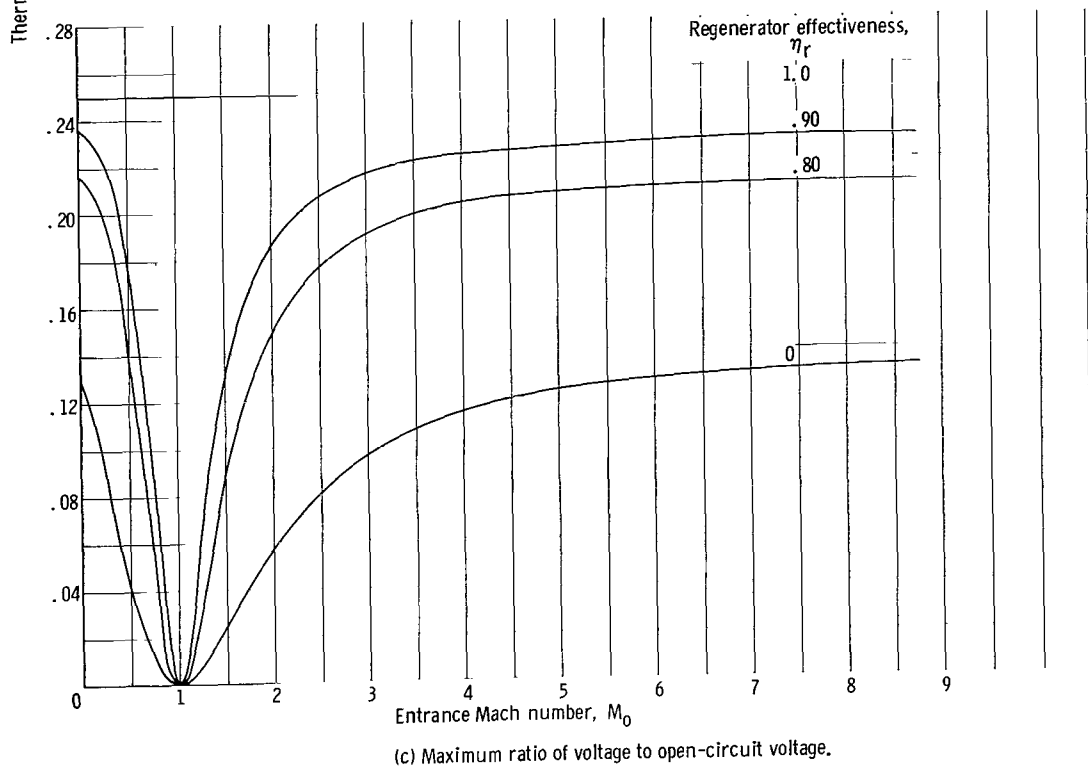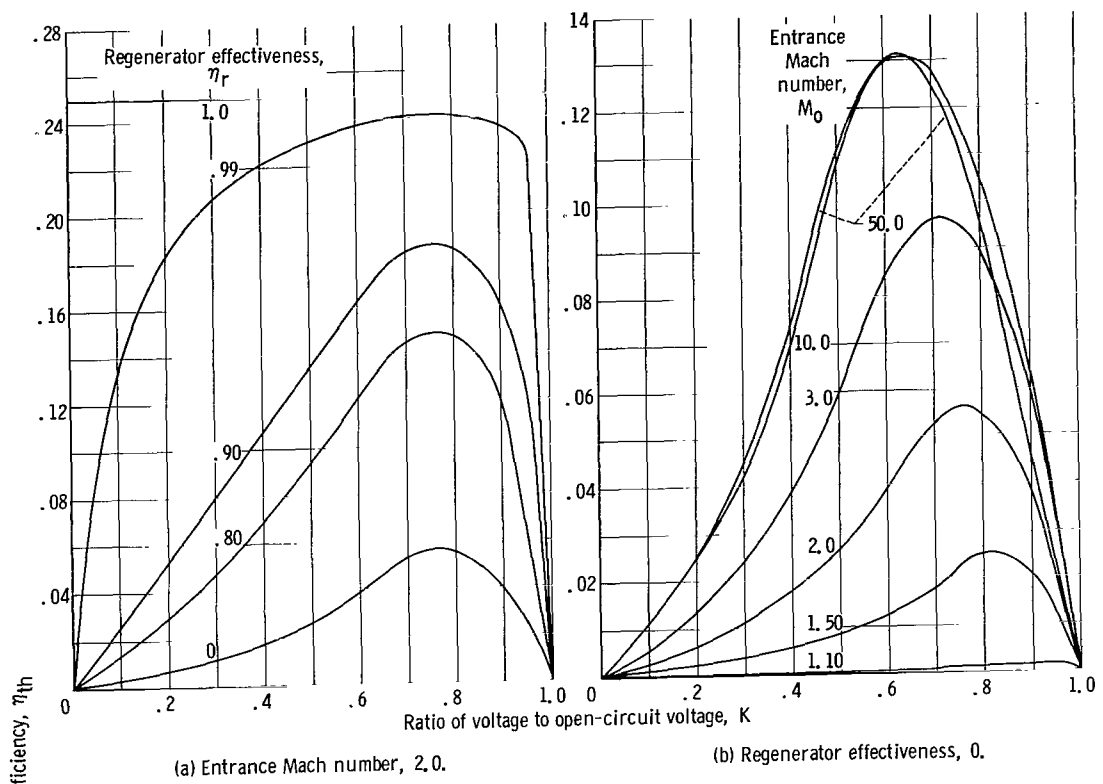
7

(a) Entrance Mach number, 2.0.

(b) Regenerator effectiveness, 0.

(c) Maximum ratio of voltage to open-circuit voltage.

Figure 3. – Thermal efficiency for limiting solution. Compressor efficiency, 0.8.

number. The value of K for which the thermodynamic efficiency is optimized is called K_{max} and is shown in figure 2.

In figure 3(c) the efficiency at $K = K_{max}$ and $\eta_{comp} = 0.8$ is plotted as a function of Mach number with regenerator effectiveness as a parameter. It can be seen that it is advantageous to operate in the region away from Mach 1, regardless of regenerator effectiveness.

In summary, it may be stated that a value of load parameter which maximizes the thermodynamic efficiency for the limiting solution has been calculated. This value is independent of the regenerator effectiveness, but dependent on Mach number, and the compressor efficiency (assumed to be 0.8 for all calculations presented herein). For the limiting solutions the efficiency is independent of the form of the electrical conductivity. Of course, the electrical conductivity of the plasma is of great practical importance in that it largely determines the generator length required to extract power, which in turn determines the output power density of the generator. It is natural, then, to use the generator output power density as a means of comparing the usefulness of various working fluids (the larger the better, of course). The conductivity to be used in the calculation of output power density is that which is determined on the basis of the theory of magnetically induced ionization. This conductivity depends on the velocity as well as the usual parameters.

DETERMINATION OF NONEQUILIBRIUM CONDUCTIVITY

Unfortunately, it is not possible to present, in closed form, an expression giving the conductivity as a function of U and K. It is true, nevertheless, that the conductivity is determined by U and K through a rather extensive system of implicit relations. The following exposition is organized in a manner paralleling the numerical computation procedure that was used to solve this system of implicit relations. The system is treated as if the electron temperature is a parameter; that is, the process is begun by assuming that the electron temperature T_e is known, then a series of relations (each calculable in terms of its predecessors) are developed, and finally, an equation for T_e is deduced. In the numerical computation, this procedure is iterated until the assumed and deduced values for T_e differ but little. The conductivity together with several other quantities of interest are readily calculated once the proper value for T_e has been found.

Degree of Ionization

In accordance with Kerrebrock (ref. 8) and more especially Lyman, et al. (ref. 11), it is assumed that the electron number density may be determined by using the Saha equation with electron temperature (rather than the gas temperature) as an argument. The validity of this procedure is discussed in reference 20.

Since the carrier gas as well as the seed gas may be ionized, it is

TABLE I. - MOLECULAR PROPERTIES USED IN CALCULATIONS

Element	Mass, kg	Polarizability, m^3	Ionization potential, ev	Statistical weights for atoms, Z_a	Statistical weights for ions, Z_i
Helium	6.645×10^{-27}	2.14×10^{-31}	24.46	1	2
Neon	3.350×10^{-26}	3.97×10^{-31}	21.47	1	6
Argon	6.631×10^{-26}	1.64×10^{-30}	15.76	1	6
Xenon	2.18×10^{-25}	4.00×10^{-30}	12.08	1	6
Cesium	2.206×10^{-25}	----------	3.89	2	1

necessary that the Saha equation be satisfied for each component. These are

$$\left.\begin{aligned}
\frac{n_e n_{s^+}}{n_s} &= \frac{Z_e Z_{s^+}}{Z_s}\left(\frac{m_e k T_e}{2\pi\hbar^2}\right)^{3/2}\exp\left(-\frac{I_s}{kT_e}\right) \\[2ex]
\frac{n_e n_{c^+}}{n_c} &= \frac{Z_e Z_{c^+}}{Z_c}\left(\frac{m_e k T_e}{2\pi\hbar^2}\right)^{3/2}\exp\left(-\frac{I_c}{kT_e}\right)
\end{aligned}\right\} \tag{23}$$

where n_{s^+}, n_s, n_{c^+}, n_c, and n_e are the local number densities of seed ions, seed atoms, carrier ions, carrier atoms, and electrons, respectively. The Z's are the statistical weights of the species: $Z_e = 2$ and $Z = (2\mathcal{L} + 1)(2\mathcal{Y} + 1)$ where $\mathcal{L}$ and $\mathcal{Y}$ are the angular momentum and spin quantum numbers, respectively. The pertinent values used for gases studied herein are given in table I. Several convenient definitions are now introduced. The local total heavy particle number density n is defined by

$$n = n_c + n_{c^+} + n_s + n_{s^+}$$

Continuity in a one-dimensional flow demands that

$$nu = n_0 u_0$$

or

$$n = \frac{n_0}{U}$$

where

$$U = \frac{u}{u_0}$$

10

and the subscript zero refers to inlet conditions. The seed ratio S is defined by

$$S \equiv \frac{n_s + n_{s+}}{n} \tag{24}$$

The degree of ionization of the components is defined by

$$X_c \equiv \frac{n_{c+}}{n_c + n_{c+}}, \qquad X_s \equiv \frac{n_{s+}}{n_s + n_{s+}} \tag{25}$$

It is now possible to write

$$n_{c+} = X_c(n_c + n_{c+}) = X_c(1 - S)n = X_c(1 - S)\frac{n_0}{U}$$

$$n_c = (1 - X_c)(n_c + n_{c+}) = (1 - X_c)(1 - S)n = (1 - X_c)(1 - S)\frac{n_0}{U}$$

$$n_{s+} = X_s(n_s + n_{s+}) = X_s S n = X_s S \frac{n_0}{U}$$

$$n_s = (1 - X_s)(n_s + n_{s+}) = (1 - X_s)S n = (1 - X_s)S \frac{n_0}{U}$$

By assuming approximate neutrality,

$$n_e = n_{c+} + n_{s+} = \left[SX_s + (1 - S)X_c \right] \frac{n_0}{U}$$

Inserting these into the Saha equations leads to the following coupled equations for X_c and X_s:

$$\frac{X_s}{1 - X_s} \left[SX_s + (1 - S)X_c \right] = \frac{U}{n_0} \frac{Z_e Z_{s+}}{Z_s} \left(\frac{m_e k T_e}{2\pi\hbar^2} \right)^{3/2} \exp\left(-\frac{I_s}{kT_e} \right)$$

$$\frac{X_c}{1 - X_c} \left[SX_s + (1 - S)X_c \right] = \frac{U}{n_0} \frac{Z_e Z_{c+}}{Z_c} \left(\frac{m_e k T_e}{2\pi\hbar^2} \right)^{3/2} \exp\left(-\frac{I_c}{kT_e} \right)$$

$$\tag{26}$$

In the numerical calculation, this pair of equations was solved by means of an iterative technique; it is possible, of course, to uncouple them and work with the resultant cubic equations.

Collision Frequencies

Having determined the degree of ionization of each species, the next step in the procedure is to determine the relevant collision frequencies. This

11

analysis accounts for elastic collisions only. The effects of inelastic colli-
sions may be crudely estimated by the inclusion of loss factors, which repre-
sent the ratio of inelastic to elastic energy losses.

The symbol ν_{AB} is used to denote the average collision frequency for
momentum transfer from species A to species B. The formulation of this report
follows that of Burgers (ref. 21), the average collision frequency being re-
lated to his friction coefficient K_{AB} by the relation

$$\nu_{AB} \equiv \frac{K_{AB}}{\mu_{AB} n_A}$$

where $\mu_{AB} = m_A m_B / (m_A + m_B)$ is the reduced mass, and n_A is the number density
of species A. Without going into elaborate detail, it should be noted that
K_{AB} (and also ν_{AB}) incorporates the complete rate of change of momentum of
species A due to collisions with species B; that is, in the momentum equation
for species A, the term $K_{AB}(\vec{u}_A - \vec{u}_B)$ represents the collision integral
$\int m_A(\vec{v}_A - \vec{u})(\delta f_A/\delta t)_{B-coll} \, d^3 v_A$. Here $\vec{v}_A$ is the particle velocity with dis-
tribution function f_A, u_A is the mean velocity of species A, and $\vec{u}$ is the
mean gas velocity.

The ν_{AB} may be expressed in terms of the monoenergetic beam cross sec-
tion $\mathscr{Q}_{AB}$ by the relation (refs. 21 and 22)

$$\nu_{AB} = n_B \sqrt{\frac{4\lambda^2}{\pi}} \left[\frac{4}{3} \lambda^{-6} \int_0^\infty \mathscr{Q}_{AB}(c) e^{-c^2/\lambda^2} c^5 \, dc \right] \tag{27}$$

where c is the relative thermal speed, $c = |\vec{c}_A - \vec{c}_B|$, $\vec{c}_A = \vec{v}_A - \vec{u}$, and

$\lambda^2 = \dfrac{2kT_A}{m_A} + \dfrac{2kT_B}{m_B}$. This definition of λ incorporates a generalization (due

to F. A. Lyman of Lewis Research Center) that allows for arbitrary species
temperature differences. For $T_A = T_B = T$, this reduces to the usual defini-
tion that is used in the references cited, $\lambda = \sqrt{2kT/\mu_{AB}}$. The quantity in
brackets is denoted by $\bar{\mathscr{Q}}_{AB}$ and may be thought of as a collision cross section
for momentum transfer averaged for a Maxwellian distribution. This quantity
corresponds to Burger's $Z_{AB}^{(11)}$ multiplied by $\sqrt{\pi/3}$ (ref. 21). This choice of a
normalizing constant is incidental and was suggested by the fact that $\sqrt{8kT/\pi m}$
is usually regarded as the average thermal speed. It should be emphasized that
ν_{AB} as defined here is not the collision frequency used to calculate the
conventional mean free path; for that quantity, the integral analogous to that
in equation (27) involves the factor c^3 rather than c^5. The higher power of
c appropriate for the momentum transfer collision frequency has the effect of
emphasizing the high energy portion of the beam cross section. In the case of
the heavy rare gases, which exhibit the Ramsauer phenomenon, this effect is of
particular importance.

For collisions involving electrons and some heavy species, it is a good approximation to take

$$\lambda = \sqrt{\frac{2kT_e}{m_e}}$$

With regard to collisions involving heavy particles, it has been assumed that the temperatures of all of the heavy species are equal; in fact, they are equal to the fluid bulk temperature T. In this case,

$$\lambda = \sqrt{\frac{2kT}{\mu_{AB}}}$$

For the collision model assumed, however, the ion-atom collision frequency turns out to be independent of the temperature (see appendix C).

The averaged electron-atom cross sections for the types of carrier and seed gases considered are plotted in figure 4 (p. 14) as functions of electron temperature. These averaged cross sections are based on equation (27) and the monoenergetic beam cross section data of reference 23.

Since coulomb effects dominate in electron-ion collisions and since consideration is restricted to singly ionized species,

$$\mathcal{Q}_{ec^+} = \mathcal{Q}_{es^+} \equiv \mathcal{Q}_{ei}$$

and the total electron-ion collision frequency is defined as

$$\nu_{ei} \equiv \nu_{ec^+} + \nu_{es^+} = (n_{c^+} + n_{s^+}) \sqrt{\frac{8kT_e}{\pi m_e}} \, \overline{\mathcal{Q}}_{ei}(T_e) = n_e \sqrt{\frac{8kT_e}{\pi m_e}} \, \overline{\mathcal{Q}}_{ei}(T_e)$$

$$(28)$$

where the last step follows from the assumption of approximate charge neutrality. In the calculation for ν_{ei} it is assumed that the usual Debye shielding theory is applicable. The resultant Maxwell averaged collision frequency may be written as (ref. 24)

$$\nu_{ei} = n_e \frac{8e^4}{3\pi^3 m_e^2 \epsilon_0^2 \left(\frac{8kT_e}{\pi m_e}\right)^{3/2}} \ln\left[\frac{3}{\sqrt{8\pi}} \left(\frac{4\pi\epsilon_0 kT_e}{e^2 n_e^{1/3}}\right)^{3/2}\right] \qquad (29)$$
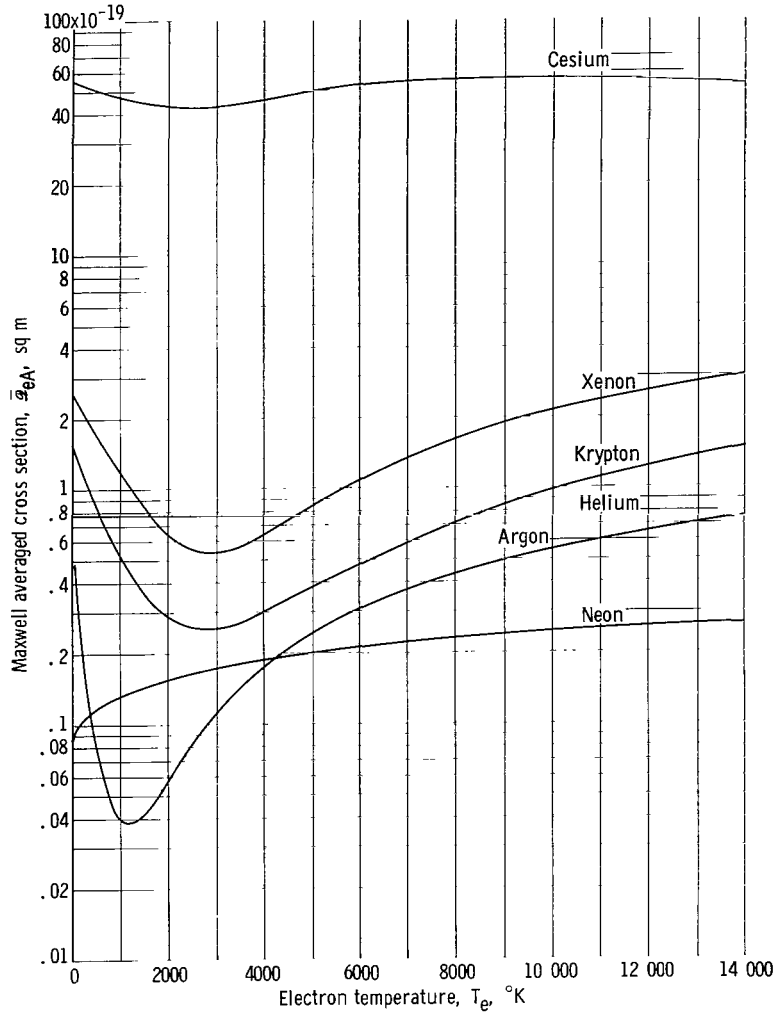
and

Figure 4. - Cross section for momentum transfer for working fluids and seed.

$$\nu_{ec^+} = \frac{n_{c^+}}{n_{c^+} + n_{s^+}} \nu_{ei}$$

$$\nu_{es^+} = \frac{n_{s^+}}{n_{c^+} + n_{s^+}} \nu_{ei}$$

To calculate ion-neutral collision frequencies it was assumed to be suffi-
cient to take account of polarization forces only, ignoring charge exchange
effects, which, of course, increase the collision frequency. Furthermore, a
simplifying assumption was made in deriving the cross section due to polariza-
tion that underestimates the true cross section for momentum transfer. This
underestimation of the ion-neutral collision frequency results in conservative
estimates of generator performance because of overestimating ion slip; there-
fore, this underestimation was felt to be tolerable.

14

As derived in appendix C, the ion-neutral collision frequency used is

$$\nu_{A^+B} = n_B \left(\frac{\pi \alpha_B e^2}{\epsilon_0 \mu_{AB}}\right)^{1/2} \tag{30}$$

where α_B is the polarizability of species B and μ_{AB} is the reduced mass $\mu_{AB} = m_A m_B/(m_A + m_B)$. For this calculation of the collision frequency the effects of charge exchange have again been neglected. This calculation is correct at low ion temperatures, but it is in error at the higher temperatures. In this report, the ion temperatures are limited to about 2000° K, for which the error will be less than 50 percent in determining the ion mobility (ref. 25). However, although the ion mobility affects the pressure at which the ion slip becomes dominant, it does not have as strong an effect on the power density. Furthermore, the error in ion mobility is in the direction that underestimates the collision frequency so that the ion slip effects as calculated become important at higher pressures than would be predicted if the charge exchange effects were included. Therefore, these calculations neglecting charge exchange are also conservative. Finally, for ion-electron collisions, noting that $\mathcal{Q}_{ei} = \mathcal{Q}_{ie}$,

$$\nu_{c^+e} = \nu_{s^+e} = \nu_{ie} = n_e \sqrt{\frac{8kT_e}{\pi m_e}} \, \overline{\mathcal{Q}}_{ei} = \nu_{ei}$$

The previous discussion shows that all of the relevant number densities and collision frequencies may be calculated if values of U and T_e are assumed.

Determination of Motion of Charged Species

For each of the species A ($A = e, c^+, s^+, c, s$) in the plasma a momentum equation of the form

$$\sum_{B \neq A} n_A \mu_{AB} \nu_{AB}(\vec{u}_A - \vec{u}_B) = n_A q_A(\vec{E} + \vec{u}_A \times \vec{B}) - \nabla p_A - m_A n_A \vec{u}_A \cdot \nabla \vec{u}_A \tag{31}$$

is considered. Higher order effects such as those associated with heat flux (ref. 21) have been ignored. In order to simplify this system the following approximations are made.

Pressure gradient and inertia terms in the equations for the charged species (e, c^+, s^+) are assumed to be small compared with the collision and electromagnetic force terms and therefore are dropped.

The motion of the neutral seed gas is assumed to be dominated by collisions with the neutral carrier gas, so that the neutral seed velocity is the

same as that of the neutral carrier gas.[1] Furthermore, by anticipating a low overall degree of ionization, the neutral species velocity is approximated by the mean (mass averaged) fluid velocity $\vec{u}$:

$$\vec{u}_s = \vec{u}_c = \vec{u}$$

These approximations allow determination of the motion of the charged species and, hence, the current density in terms of the mean velocity. The resultant expression for the current (Ohm's law) together with the equations (1) to (4) constitute a complete system determining the fluid dynamic variables u, ρ, P, h, and the current density j. Incidentally, the momentum equation for the fluid as a whole (eq. (2)) results from summing the individual species momentum equations; the collision terms, of course, cancel in pairs.

In order to further simplify the system, the seed and carrier ions are assumed to move with the same velocity $\vec{u}_i$:

$$\vec{u}_{s+} = \vec{u}_{c+} = \vec{u}_i$$

The ion momentum may then be described by a single equation consisting of the weighted sum of the equations for the seed ion s^+ and the carrier ions c^+ with the weights being $n_{s+}/(n_{s+} + n_{c+})$ and $n_{c+}/(n_{s+} + n_{c+})$, respectively. In justification of this approximation, it may be observed that the formulation is exact in the limits $n_{s+}/n_{c+} \to 0$ and $n_{c+}/n_{s+} \to 0$. Also, since ion-ion collisions are governed by the long-range coulomb interaction, the ion-ion cross section is very large so that above a certain degree of ionization the ions are locked together, so to speak.

Finally, as discussed in the section dealing with the collision frequencies,

$$\nu_{s^+e} \approx \nu_{c^+e} = \nu_{ei}$$

$$\nu_{es^+} + \nu_{ec^+} = \nu_{ei}$$

$$\mu_{es} \approx \mu_{ec} = m_e$$

The resultant equations for electrons and ions are

$$m_e(\nu_{ec} + \nu_{es})(\vec{u}_e - \vec{u}) + m_e\nu_{ei}(\vec{u}_e - \vec{u}_i) = -e(\vec{E} + \vec{u}_e \times \vec{B}) \qquad (32a)$$

---

[1]This simplification could lead to underestimation of ion slip in cases where the seed possesses a very large polarizability. In this situation the strongly interacting seed neutrals and ions might well slip together through the carrier neutrals. In order to avoid this difficulty while retaining simplicity, in such cases the seed gas is assigned a ficticious polarizability equal to that of the carrier gas.

$$\left[\frac{n_{c^+}}{n_{c^+} + n_{s^+}}\left(\mu_{cc}\nu_{c^+c} + \mu_{cs}\nu_{c^+s}\right) + \frac{n_{s^+}}{n_{c^+} + n_{s^+}}\left(\mu_{cs}\nu_{s^+c} + \mu_{ss}\nu_{s^+s}\right)\right]$$

$$\cdot \left(\vec{u}_i - \vec{u}\right) + m_e\nu_{ei}\left(\vec{u}_i - \vec{u}_e\right) = e\left(\vec{E} + \vec{u}_i \times \vec{B}\right) \qquad (32b)$$

By defining the transverse direction ($\perp$) as the direction of $\vec{u} \times \vec{B}$ and the parallel direction ($\parallel$) as that of $\vec{u}$, the solution to the system of equations (32) may be written as

$$\left.\begin{aligned}
u_{e\perp} &= -\Theta_e\left(u + \frac{E_\perp}{B}\right) + \Omega_e\frac{E_\parallel}{B} \\[2mm]
u_{e\parallel} &= u - \Theta_e\frac{E_\parallel}{B} - \Omega_e\left(u + \frac{E_\perp}{B}\right) \\[2mm]
u_{i\perp} &= \Theta_i\left(u + \frac{E_\perp}{B}\right) + \Omega_i\frac{E_\parallel}{B} \\[2mm]
u_{i\parallel} &= u + \Theta_i\frac{E_\parallel}{B} - \Omega_i\left(u + \frac{E_\perp}{B}\right)
\end{aligned}\right\} \qquad (33)$$

where

$$\left.\begin{aligned}
\Theta_e &\equiv G^{-1}\left[\nu_{in}^2\nu_{en} + \nu_{in}\nu_{ei}\left(\nu_{in} + \nu_{en}\right) + \nu_{en}\omega_e^2\right]\omega_e \\[2mm]
\Omega_e &\equiv G^{-1}\left[\nu_{in}^2 + \nu_{ei}\left(\nu_{in} + \nu_{en}\right) + \omega_e^2\right]\omega_e^2 \\[2mm]
\Theta_i &\equiv G^{-1}\left[\nu_{en}^2\nu_{in} + \nu_{en}\nu_{ei}\left(\nu_{en} + \nu_{in}\right) + \nu_{in}\omega_e^2\right]\omega_e \\[2mm]
\Omega_i &\equiv G^{-1}\left[\nu_{en}^2 + \nu_{ei}\left(\nu_{en} + \nu_{in}\right) + \omega_e^2\right]\omega_e^2
\end{aligned}\right\} \qquad (34)$$

and where

$$G \equiv \left[\nu_{in}\nu_{en} + \nu_{ei}\left(\nu_{in} + \nu_{en}\right)\right]^2 + \left[\nu_{in}^2 + \nu_{en}^2 + 2\nu_{ei}\left(\nu_{in} + \nu_{en}\right) + \omega_e^2\right]\omega_e^2$$

$$\nu_{in} \equiv \frac{1}{m_e}\left[\left(\frac{n_{c^+}}{n_{c^+} + n_{s^+}}\right)\left(\mu_{cc}\nu_{c^+c} + \mu_{cs}\nu_{c^+s}\right) + \left(\frac{n_{s^+}}{n_{c^+} + n_{s^+}}\right)\left(\mu_{cs}\nu_{s^+c} + \mu_{ss}\nu_{s^+s}\right)\right]$$

$$\nu_{en} \equiv \nu_{ec} + \nu_{es}$$

$$\omega_e \equiv \frac{eB}{m_e}$$

17

The coefficients Θ are related to the direct response to an electric field, while the Ω's are related to the precessional response to crossed electric and magnetic fields. The quantity ν_{in} is a hybrid ion collision frequency modified by a mass ratio. When no seed is present, ν_{in} reduces to

$$\frac{\mu_{cc}}{m_e} \nu_{c^+c} = \frac{1}{2} \frac{m_c}{m_e} \nu_{c^+c}$$

If the carrier gas is not appreciably ionized, however,

$$\nu_{in} = \frac{\mu_{cs}}{m_e} \nu_{s^+c} + \frac{\mu_{ss}}{m_e} \nu_{s^+s}$$

The phenomenological equation for the current (Ohm's law) for the segmented Faraday generator can be determined from equation (33).

Power Delivered to Electrons

The current in a segmented Faraday generator must first be determined. When the electrodes are segmented, no axial current flows; $j_{\parallel} = 0$. If $n_e = n_i$, $u_{e\parallel} = u_{i\parallel}$. Then from equation (33)

$$\frac{E_{\parallel}}{B} = -\frac{\Omega_e - \Omega_i}{\Theta_e + \Theta_i} \left(u + \frac{E_{\perp}}{B} \right) \tag{35a}$$

which may be written by the use of equation (34) as follows:

$$E_{\parallel} = -\frac{\left(1 - \dfrac{\nu_{en}}{\nu_{in}}\right)\left(\dfrac{\omega_e}{\nu_{en} + \nu_{ei}}\right)}{1 + \dfrac{\nu_{en}}{\nu_{in}}\left(\dfrac{\nu_{ei}}{\nu_{en} + \nu_{ei}}\right) + \left(\dfrac{\omega_e}{\nu_{en} + \nu_{ei}}\right)\dfrac{\omega_e}{\nu_{in}}} (U - K)u_0 B \tag{35b}$$

For $\nu_{en}/\nu_{in} \ll 1$,

$$E_{\parallel} \simeq -\frac{\beta_e}{1 + \beta_e \beta_i} (U - K)u_0 B$$

where β_e and β_i, the electron and ion Hall parameters, respectively, are

$$\beta_e = \frac{\omega_e}{\nu_{en} + \nu_{ei}}$$

$$\beta_i = \frac{\omega_e}{\nu_{in}}$$

18

Equation (35a) may be used in equation (33) to determine $u_{e\perp}$ and $u_{i\perp}$ so that $j_\perp = en_e(u_{i\perp} - u_{e\perp})$ can be written as follows:

$$j_\perp = en_e\left[\frac{(\Theta_e + \Theta_i)^2 + (\Omega_e - \Omega_i)^2}{\Theta_e + \Theta_i}\right]\left(u + \frac{E_\perp}{B}\right) \tag{36}$$

which may, after reduction using equation (34), be written as

$$j_\perp = en_e\left[\frac{(\nu_{in} + \nu_{en})\omega_e}{\nu_{in}\nu_{en} + \nu_{ei}(\nu_{in} + \nu_{en}) + \omega_e^2}\right]\left(u + \frac{E_\perp}{B}\right) \tag{37}$$

or, by rearranging and inserting $U = u/u_0$ and $K \equiv -E_\perp/u_0 B$,

$$j_\perp = \frac{n_e e^2}{m_e(\nu_{en} + \nu_{ei})}\left[\frac{1 + \dfrac{\nu_{en}}{\nu_{in}}}{1 + \dfrac{\nu_{en}}{\nu_{in}}\left(\dfrac{\nu_{ei}}{\nu_{ei} + \nu_{en}}\right) + \left(\dfrac{\omega_e}{\nu_{en} + \nu_{ei}}\right)\dfrac{\omega_e}{\nu_{in}}}\right](U - K)u_0 B \tag{38}$$

Thus, the effective conductivity σ is given by

$$\sigma = \frac{n_e e^2}{m_e(\nu_{en} + \nu_{ei})}\left[\frac{1 + \dfrac{\nu_{en}}{\nu_{in}}}{1 + \dfrac{\nu_{en}}{\nu_{in}}\left(\dfrac{\nu_{ei}}{\nu_{ei} + \nu_{en}}\right) + \left(\dfrac{\omega_e}{\nu_{en} + \nu_{ei}}\right)\dfrac{\omega_e}{\nu_{in}}}\right] \tag{39a}$$

For $\nu_{en}/\nu_{in} \ll 1$ this reduces to the familiar form

$$\sigma \simeq \frac{n_e e^2}{m_e(\nu_{en} + \nu_{ei})}\left(\frac{1}{1 + \beta_e\beta_i}\right) \tag{39b}$$

In equations (39a) and (39b) for σ, the leading factor is the usual expression for conductivity; the quantity in brackets may be thought of as accounting for ion slip.

An energy balance for the electron species will presently be considered, and for this the rate at which electrons acquire energy by virtue of their motion in the electric field must be determined. This rate cannot be defined in a completely unambiguous way, but rather depends on the frame of reference in which the calculation is carried out. The frame of reference that will be used moves with the mean (mass averaged) fluid velocity. This choice eliminates the need to take account of directed energy in the calculation of the energy lost by electrons in collisions with the heavy species; consequently,

the energy lost is simply proportional to the difference in species temperatures. An asterisk is used to denote vectors reckoned in this frame of reference. Thus, to find the power $\mathscr{P}_e$ delivered to the electrons in a unit of volume, it is necessary to calculate

$$\mathscr{P}_e = n_e \vec{u}_e^* \cdot (-e\vec{E}^*) \tag{40}$$

where

$$\vec{u}_e^* = \vec{u}_e - \vec{u}$$

$$\vec{E}^* = \vec{E} + \vec{u} \times \vec{B}$$

From equation (33),

$$u_{e\perp}^* = -\Theta_e\left(u + \frac{E_\perp}{B}\right) + \Omega_e\frac{E_\parallel}{B}$$

$$u_{e\parallel}^* = -\Theta_e\frac{E_\parallel}{B} - \Omega_e\left(u + \frac{E_\perp}{B}\right)$$

and

$$E_\perp^* = E_\perp + uB$$

$$E_\parallel^* = E_\parallel$$

By straightforward substitution,

$$\mathscr{P}_e = en_e u^2 B\Theta_e\left[\left(1 + \frac{E_\perp}{uB}\right)^2 + \left(\frac{E_\parallel}{uB}\right)^2\right] \tag{41}$$

For the segmented Faraday generator equation (35a) may be used to give $E_\parallel$ in terms of $E_\perp + uB$, and $\mathscr{P}_e$ may be written as

$$\mathscr{P}_e = en_e u^2 B\Theta_e\left[1 + \left(\frac{\Omega_e - \Omega_i}{\Theta_e + \Theta_i}\right)^2\right]\left(1 + \frac{E_\perp}{uB}\right)^2$$

Inserting the definitions given in equation (34) leads, after reduction, to

$$\mathscr{P}_e = n_e m_e(\nu_{en} + \nu_{ei})\beta_e^2\psi(U - K)^2 u_0^2 \tag{42}$$

where

20

$$\psi \equiv \frac{1 + \dfrac{\nu_{en}}{\nu_{in}}\left(\dfrac{\nu_{ei}}{\nu_{ei} + \nu_{en}}\right) + \dfrac{\nu_{en}}{\nu_{in}}\left(\dfrac{\omega_e}{\nu_{en} + \nu_{ei}}\right)\dfrac{\omega_e}{\nu_{in}}}{\left[1 + \dfrac{\nu_{en}}{\nu_{in}}\left(\dfrac{\nu_{ei}}{\nu_{ei} + \nu_{en}}\right) + \left(\dfrac{\omega_e}{\nu_{en} + \nu_{ei}}\right)\dfrac{\omega_e}{\nu_{in}}\right]^2}$$ (43)

For $\nu_{en}/\nu_{in} \ll 1$, ψ reduces to

$$\psi = \left(\frac{1}{1 + \beta_e \beta_i}\right)^2$$ (44)

When equations (38) to (44) are used, $j_\perp$ and $\mathcal{P}_e$ may be calculated for any assumed values of U and T_e.

Energy Balance for Electrons

The assumption made here is that at every point in the flow the rate at which electrons acquire energy from the electric field is exactly balanced by the rate at which they lose energy to the other species by collisions. The former rate has just been calculated; the latter is

$$\mathcal{P}_e' = n_e \sum_{j \neq e} \tilde{\nu}_{ej}\left(\frac{3}{2} kT_e - \frac{3}{2} kT_j\right)$$ (45)

where $\tilde{\nu}_{ej}$ is the collision frequency for energy transfer. Now for elastic collisions between a light particle e and a heavy particle j, this collision frequency is given to very good approximation by

$$\tilde{\nu}_{ej} = \frac{2m_e}{m_j} \nu_{ej}$$

where ν_{ej} is the collision frequency for momentum transfer. In order to account (very crudely) for inelastic collisions, loss factors δ_{ej} may be introduced as follows:

$$\tilde{\nu}_{ej} = \frac{2m_e}{m_j} \delta_{ej}\nu_{ej}$$

It is also assumed that $T_j = T$ for all the heavy species. Thus,

$$\mathcal{P}_e' = 3n_e m_e(kT_e - kT) \sum_{j \neq e} \nu_{ej} m_j^{-1}\delta_{ej} = 3n_e m_e(\nu_{en} + \nu_{ei})(T_e - T)\frac{k}{m}\Delta$$ (46)

21

where $\overline{m}$ is the average mass of the heavy particles, $\overline{m} = (1 - S)m_c + Sm_s$ (again $m_{c^+} = m_c$ and $m_{s^+} = m_s$), and $\triangle$ is a composite loss factor:

$$\triangle \equiv \sum_{j \neq e} \frac{\nu_{ej}}{\nu_{en} + \nu_{ei}} \left(\frac{\overline{m}}{m_j}\right) \delta_{ej} \tag{47}$$

Equating the previous expression for $\mathscr{G}_e'$ to that for $\mathscr{G}_e$ from equation (42) results in

$$T_e = T + \frac{u_0^2}{\left(\frac{k}{\overline{m}}\right)} \frac{1}{3\triangle} \beta_e^2 \psi (U - K)^2$$

Now

$$T = \gamma M_0^2 T_0 UP$$

$$\frac{u_0^2}{\left(\frac{k}{\overline{m}}\right)} = \gamma M_0^2 T_0$$

The equation used to determine the electron temperature may then be written as

$$T_e = \gamma M_0^2 T_0 \left[UP + \frac{1}{3\triangle} \beta_e^2 \psi (U - K)^2 \right] \tag{48}$$

For all calculations made herein $\triangle$ was calculated with $\delta_{ej} = 1$ for all j. This procedure is valid for monatomic gases and for reasonably low electron temperatures so that the calculations are consistent. The difficulty with this procedure really stems from the fact that an elevated electron number density corresponding to the elevated electron temperature can be realized only by inelastic ionizing collisions. It is assumed that this will be a small part of the energy balance for the entire swarm of electrons. This may indeed be the case, except for the fact that for this elevated electron temperature there will be recombination, and the energy that the electron must lose when it recombines may be lost - not to the remaining swarm of electrons but possibly to the walls by radiation (ref. 26). This effect diminishes as the electron temperature increases because of superelastic collisions and as the optical path increases because of absorption of the radiation in the body of the gas.

Since $\triangle$, β_e, and ψ depend on U and T_e, equation (48) may be viewed as an implicit relation defining T_e as a function of U (P is a function of U alone).

Since $T_e(U)$ is determined, it is now possible to calculate $\sigma(U, T_e)$, using equation (39), and hence the value of $\Sigma = \sigma/\sigma_0$ required in equation (15) (σ_0 is the conductivity at the entrance where $U = 1$).

CRITERIA FOR COMPARING GENERATORS

The analytical model developed herein may be used to calculate the operating characteristics of the generator, provided that the numerous operating parameters have been fixed. These include the nature of the working fluid (the carrier gas and seed material used), the relative load voltage, the magnetic field intensity, and the inlet conditions (total temperature, pressure, and Mach number).

One of the primary purposes of this analysis is to afford some basis for comparing the merits of various working fluids. It seems reasonable to expect that such a comparison will possess a validity which transcends the limitations of the present model (e.g., constant cross section duct). In any event, for a given working fluid, it is necessary to decide in some logical fashion how to set the values of the other operating parameters. In fact, in view of the large number of parameters, it is highly desirable to eliminate from consideration as many of these parameters as possible. In the present work this was accomplished, when possible, by fixing certain parameters at values that optimize generator performance.

Of course, the criteria which one uses in estimating generator performance depend on the task that the generator is to accomplish. In the present work, it has been assumed that the generator is to provide electric power for a space vehicle. This means that low weight is of primary importance. In space, heat rejection must be accomplished by means of a radiator, and it turns out that the radiator weight is always important and frequently dominates the total system weight. Assuming that radiator weight is proportional to radiator area, it is reasonable to impose the restriction of minimum radiator area. This restriction is treated in detail in appendix B, the main result being an expression (eq. (B11)) for the thermodynamic cycle efficiency satisfying the minimum area condition.

With the question of ground rules settled, it is now possible to identify the thermodynamic cycle efficiency as the primary measure of generator performance. The efficiency is primarily a function of the generator conversion effectiveness, which, in turn, depends in an involved manner on all of the generator parameters, unless one considers the limiting case of an infinite interaction length ξ (usually called the interaction parameter since it is dimensionless). In the limiting case the conversion effectiveness is found to be dependent only on the entrance Mach number and the relative load voltage K. The temptation is to fix the value of the relative load voltage by optimizing the thermodynamic cycle efficiency using the limiting expression for conversion effectiveness. Now the use of the limiting expression is, in a sense, unreasonable, since it corresponds to a generator of infinite length. The following modifications were introduced to avoid this difficulty. The optimizing procedure gives, in addition to optimum values for relative load voltage and thermodynamic cycle efficiency, an optimum value for the conversion effectiveness. In the supersonic regime, the value of relative load voltage is reasonable, but an infinite length is required to achieve the maximum conversion effectiveness. In this case, the actual generator length was taken to be that length required to achieve 90 percent of the maximum value. In the subsonic

regime, the optimizing procedure yields a relative load voltage of unity, corresponding to open-circuit conditions, and choking at infinity. Any reduction of the relative load voltage results in choking at a finite length. In this case, the relative load voltage was relaxed to a value of nine-tenths, and the actual generator length taken to be that at which choking occurred. By this procedure, the relative load voltage was eliminated as a free parameter by specifying it to have that value which maximizes the thermodynamic cycle efficiency.

In order to fix additional parameters, the output power density was considered as a measure of generator performance. The parameters fixed by optimizing power output density are pressure and seed fraction. Actually, either the pressure or the magnetic field intensity can be fixed. (It turns out that pressure and field intensity are linearly related at optimum conditions, the power output density being a monotonic function of either.) The magnetic field intensity was left as a free parameter to insure that reasonable values thereof were considered. Since both the efficiency and power output density are strictly increasing functions of total temperature, this parameter was fixed by choosing for it a not too unreasonably high value, namely 4000° R (2222° K). Thus, all but two (magnetic field intensity and Mach number) of the operating parameters were fixed.

Some further remarks regarding pressure and seed fraction are in order. For particular values of magnetic field and Mach number, it is clear that an optimum pressure exists. At very high pressures, the conductivity and the power output density decrease (because of electron-neutral collisions) with increasing pressure faster than the available energy increases. At low pressures not only does the available energy decrease with decreasing pressure, but also the conductivity decreases because of ion slip. Judging from the calculations performed, it appears that the ion slip effect is of dominant importance. With respect to the type of seed used, calculations show cesium (because of its very low ionization potential) to possess a clear-cut advantage over the lighter alkali metals and thallium. Only the results with cesium as seed material are therefore presented. Again for particular values of the free parameters (magnetic field intensity and Mach number), an optimum value for seed fraction exists, at least for the generator model considered. For practical values of magnetic field, it turns out that for any noble carrier gas and no seed the plasma still behaves over most of the duct length as a partially ionized gas; that is, electron-neutral collisions are still important, so that the conductivity increases with the electron number density. Thus, increasing the seed fraction from zero improves the output power density. The addition of seed, however, always has the effect of lowering the electron temperature for reasons that may be traced to the very large elastic scattering cross sections of appropriate seed materials. Although the results are not presented, thallium seeding was investigated just because of its relatively low cross section. As is obvious from the Saha equation, lowering the electron temperature has the effect of lowering the fraction of seed ionized. In adding seed, then, a point is reached at which the gain in electron number density that would be expected from having made available more seed to be ionized is just cancelled by the reduction of the fraction of seed ionized. Beyond this point, of course, addition of seed material is detrimental to the output power density.

24
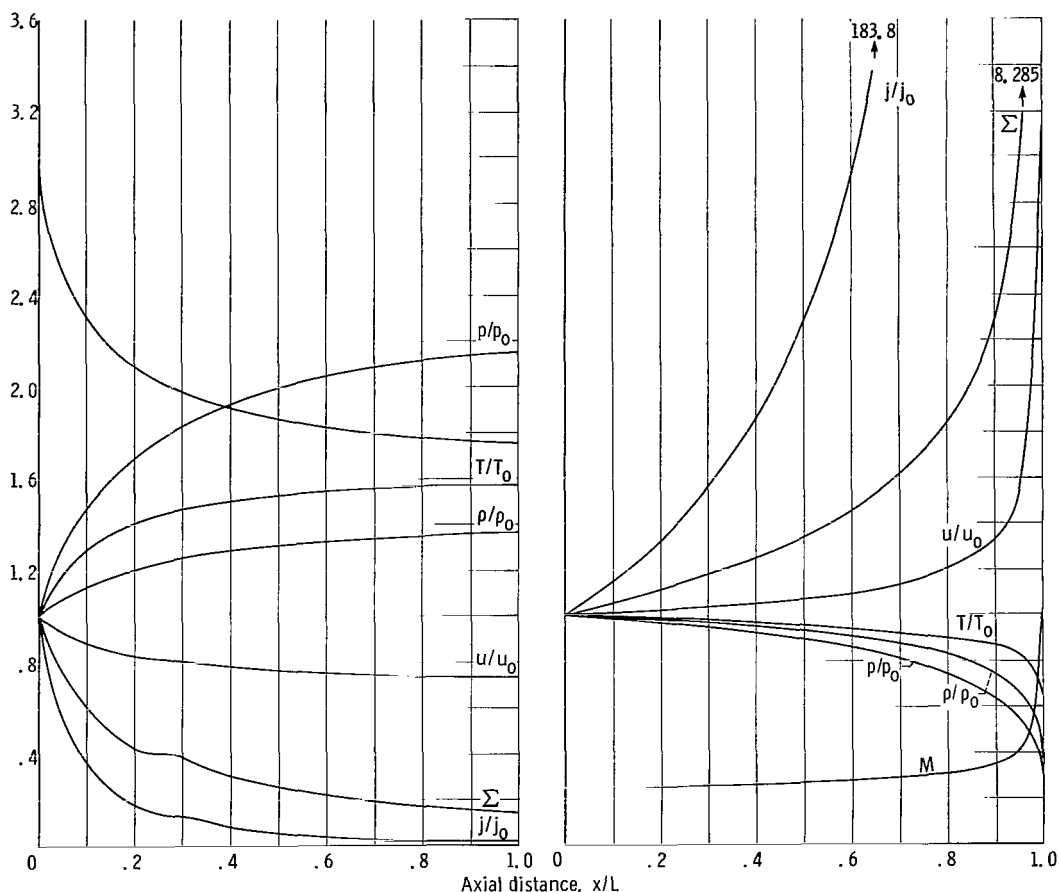
(a) Supersonic flow. Magnetic field strength, B, 2.0 webers per square meter; entrance temperature, T_0, 555° K; entrance pressure, P_0, 5.12×10^3 newtons per square meter; entrance fluid velocity, u_0, 1316 meters per second; entrance electrical conductivity, σ_0, 701.1 mhos per meter; entrance current density, j_0, 5.463×10^5 amperes per square meter; seed ratio, S, 3.6×10^{-4}; entrance density, ρ_0, 0.0443 kilogram per cubic meter.

(b) Subsonic flow. Magnetic field strength, B, 2.0 webers per square meter; entrance temperature, T_0, 2175° K; entrance pressure, P_0, 3.874×10^4 newtons per square meter; entrance fluid velocity, u_0, 217.1 meters per second; entrance electrical conductivity, σ_0, 107.2 mhos per meter; entrance current density, j_0, 4.658×10^3 amperes per square meter; seed ratio, S, 4.51×10^{-4}; entrance density, ρ_0, 0.0813 kilogram per cubic meter.

Figure 5. – Typical solution for generator.

RESULTS AND DISCUSSION

All calculations of output power density are made for the optimum conditions outlined previously. The optimum K, called K_{max}, is shown in figure 2 (p. 7). The determination of the optimum seed and pressure was done numerically. The seed fraction and pressure were varied systematically until the maximum power density was found. These calculations were carried out using an IBM 7094 computer.

Calculations are made for helium, neon, argon, and xenon with cesium seed. Other seed materials were considered and found to be inferior to cesium. The atomic constants used in the calculations are shown in table I (p. 10). A typical solution is shown in figure 5(a) for argon at Mach 3.0 and B of 2.0 webers per square meter. The only unusual behavior is in the conductivity
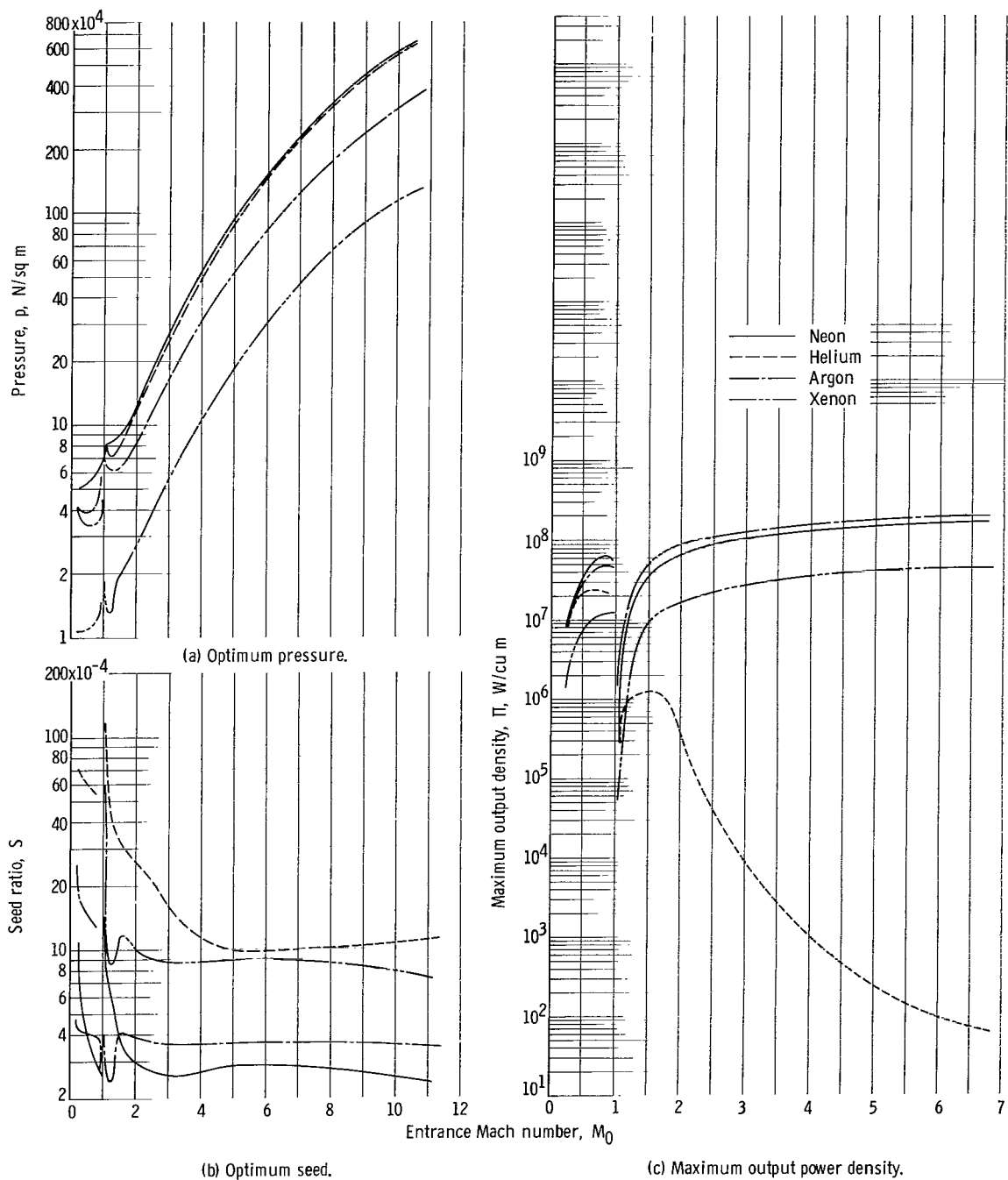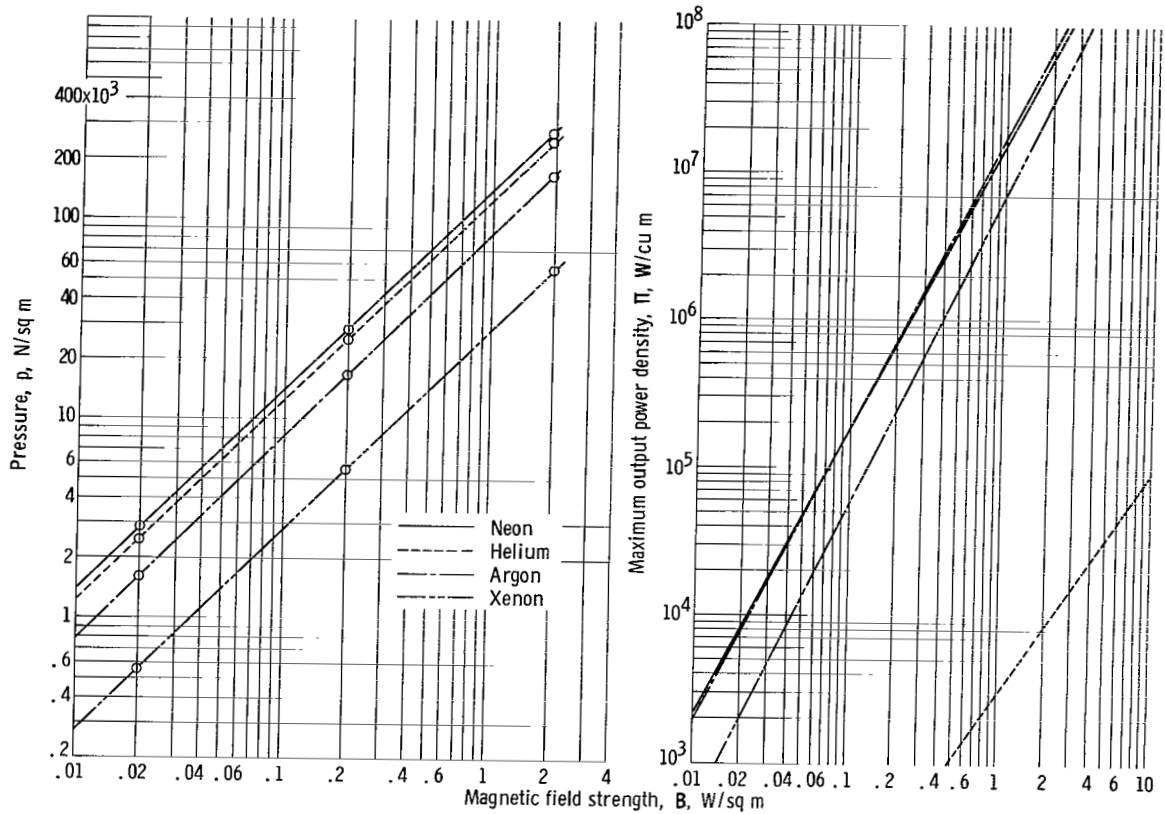
(a) Optimum pressure.

(b) Optimum seed.

(c) Maximum output power density.

Figure 6. - Solutions for magnetic field strength of 2.0 and maximum ratio of voltage to open-circuit voltage (i. e., $K = K_{max}$).

variation. In the region for x/L less than 0.2 the seed is fully ionized so
that the carrier ionization contributes to the conductivity. At x/L = 0.2,
the carrier ionization becomes insignificant and the conductivity is determined
from the seed ionization only. This results in a less steep variation of con-
ductivity with x/L. A typical example for a subsonic duct is shown in fig-
ure 5(b) for argon at a magnetic field strength of 2.0 and a Mach number of
0.25. The variables behave in the inverse manner compared to the supersonic
case.

The curves in figure 6 for the constant magnetic field at 2.0 webers per
square meter show that the optimum pressure generally increases with Mach num-
ber (fig 6(a)) and the optimum seed generally decreases (fig. 6(b)). The power
density (fig 6(c)) reaches a peak in the subsonic Mach number region, decreases
at sonic velocity, and again increases with supersonic Mach number. Because of
the discontinuous change in K, the low supersonic Mach number power densities
are lower than the high subsonic Mach number power densities. It can be seen
that argon and neon are the best; argon is slightly better in the supersonic
region and neon slightly better in the subsonic region. Xenon is not quite as
good as either, while helium is inferior, especially at the high supersonic
Mach number. As a matter of fact, at Mach numbers greater than 1.5 the power
density for the helium carrier begins to decrease. This anomalous behavior can
be attributed to the much higher elastic cross section for momentum transfer
and the large ionization potential.

The results in figure 7 (p. 28) are for a fixed entrance Mach number of
3.0, and they show that optimum pressure, seed fraction, and maximum power den-
sity increase with magnetic field. For small magnetic fields neon becomes the
best working fluid, as the field increases argon becomes the best, and at very
high fields xenon may become superior. Helium is inferior, except possibly at
impractically small magnetic fields and power densities.

It is possible to compare the constant area generator to a constant ve-
locity generator by means of equation (19) both for constant and variable con-
ductivity. This comparison is made in figure 8(a) (p. 29) for subsonic and
figure 8(b) for supersonic Mach numbers. The comparison for constant conduc-
tivity can be used to illustrate the effects of the constant area insofar as
this restriction causes the velocity to change. For subsonic flow, the power
density for the constant area generator is greater and for supersonic flow it
is less than for the constant velocity case. The effect of the variation in
the conductivity can be seen from these calculations by comparing the results
for the various working fluids with those for the case where conductivity is
assumed constant at the inlet value. With this comparison, it is possible to
talk about an average conductivity for the working fluid in the variable con-
ductivity calculation. In the case of subsonic flow, the average conductivity
is increased at lower Mach numbers, except for helium. At the very low sub-
sonic Mach numbers the electron temperature is not elevated above the gas tem-
perature for helium, primarily because the mobility of the electron is so small
that the factor β_e^2 in equation (48) does not contribute to the electron tem-
perature. Hence, the average conductivity not only is lower than that for
other gases, but also lower than that for a constant conductivity at the en-
trance value. This occurs because the static temperature is decreasing in the

(a) Optimum pressure.

(c) Maximum output power density.
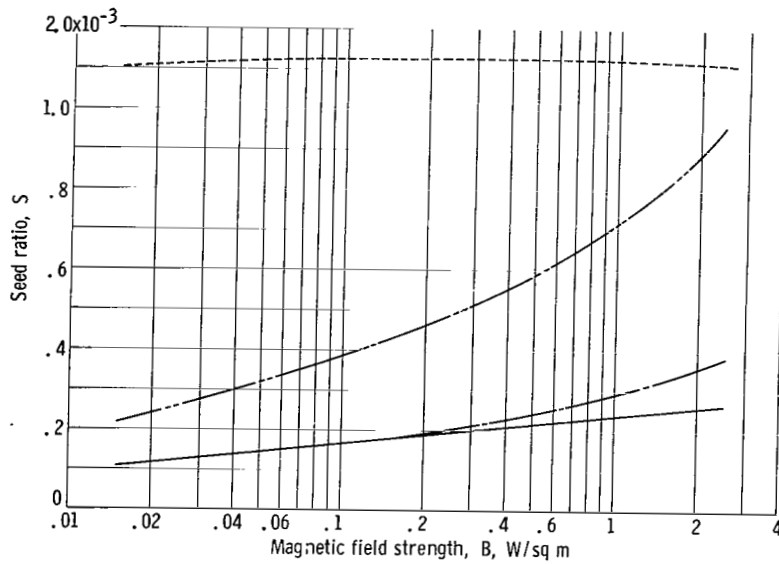
(b) Optimum seed.

Figure 7. - Solutions for entrance Mach number of 3.0 and maximum ratio of voltage to open-circuit voltage (i. e., $K = K_{max}$).

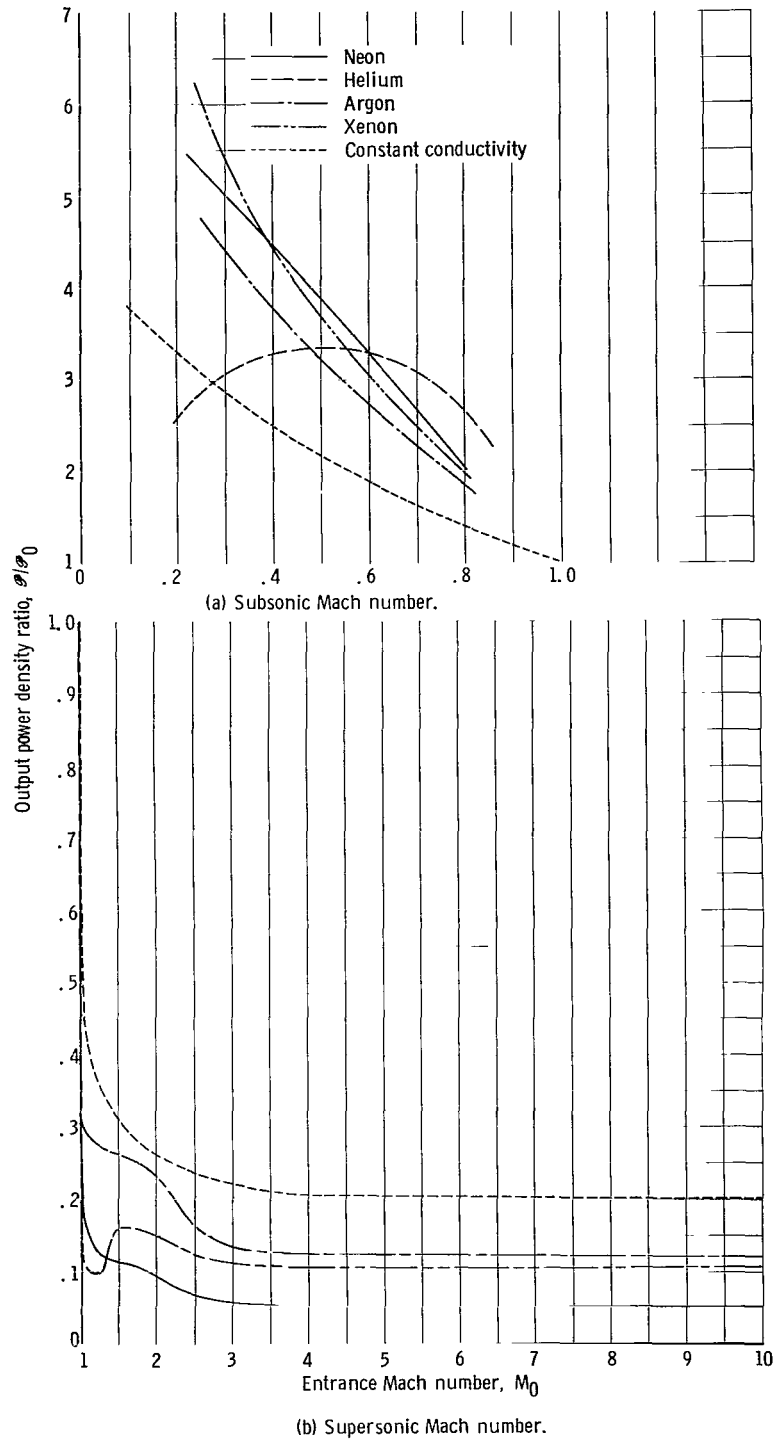(a) Subsonic Mach number.

(b) Supersonic Mach number.

Figure 8. – Power density ratio defined in equation (19) for magnetic field strength of 2.0 and maximum ratio of voltage to open-circuit voltage ($K = K_{max}$).

axial direction.

For the supersonic cases, the average conductivity for all gases is always less than the entrance conductivity. Helium has an average conductivity that is at least an order of magnitude less than all other working fluids. This is another manifestation of the high collision cross section of the neutral helium atoms and large ionization potential.

CONCLUDING REMARKS

The following conclusions can be drawn from this study of Brayton cycle magnetohydradynamic power generation with nonequilibrium conductivity:

1. Thermal efficiency changes little for Mach numbers greater than 3.0 in the supersonic case, but it decreases monotonically with increasing values for the subsonic case.

2. Optimum pressures generally decrease with increasing molecular weight, whereas optimum seed generally is lowest for neon and argon. The optimum value of seed fraction was always less than 0.0005 for argon and cesium.

3. Optimum power densities change little for Mach numbers greater than 3.0 (except for helium) in the supersonic case, and they increase in the subsonic region to a maximum at Mach 1.0. When considering power density and efficiency, it seems that Mach 3.0 is a good operating point for the supersonic region, and Mach 0.5 for the subsonic. Argon is the best in the supersonic region, and neon the best in the subsonic region.

4. The optimum seed, pressure, and power density increase with increasing magnetic field strength; consequently, it is desirable to have as large a field strength as possible.

5. The average conductivity is highest for neon and xenon in the subsonic region, and for argon in the supersonic region.

Lewis Research Center,
    National Aeronautics and Space Administration,
        Cleveland, Ohio, December 2, 1964.

APPENDIX A

SYMBOLS

A_e electrode area

A_r radiator area

a,b machine efficiency parameters

B magnetic field strength

b_0 impact parameter

c particle speed

$E_{\parallel}, E_{\perp}$ components of electric field, defined on p. 17

$\vec{E}^*, E_{\parallel}^*, E_{\perp}^*$ electric field and components in coordinates moving with particle

$\vec{E}_1, \vec{E}_2$ electric fields

e electron charge

$\vec{F}$ force

G collision parameter

$\vec{g}$ dipole moment

H height of electrodes

h enthalpy

$\hbar$ Planck constant

I ionization potential

$\hat{\hat{I}}$ unit dyad

$j, j_{\parallel}, j_{\perp}$ current density and components parallel and perpendicular to magnetic field

K ratio of voltage to open-circuit voltage

K_1 load voltage parameter, defined on p. 4

K_{∞} ratio of voltage to open-circuit voltage for infinitely long duct

k Boltzman's constant

L	generator length
M	Mach number
M_O	entrance Mach number, defined on p. 4
M_1	Mach number parameter, defined on p. 4
m_e, m_c, m_s	mass of electron, carrier atom, and seed atom
n	total number density
n_e	electron number density
n_s, n_c	seed neutral and carrier neutral number density
n_{s+}, n_{c+}	seed ion and carrier ion number density
P	nondimensional pressure, defined on p. 4
$\mathscr{P}$	output power density
$\mathscr{P}_e, \mathscr{P}_e'$	power density delivered to and lost by electrons
p	pressure
Q	heat
$\bar{\mathscr{D}}_{AB}$	average cross section for momentum transfer
q	charge
R_L	load resistance
r	radius
$\hat{r}_1$	$\vec{r}_1 / r_1$
S	seed ratio
s	entropy
T_{ave}	average temperature
T_e	electron temperature

$T_1, T_2, T_{2'},$
$T_3, T_4, T_5,$ } thermodynamic cycle temperature
$T_{5'}, T_6$

t   time

U   nondimensional fluid velocity, defined on p. 4

U_{ch} choking velocity

u   fluid velocity

$\vec{u}, \vec{u}_i$ neutral and ion velocities

$\vec{u}_e^*$ relative velocity of electrons

$u_{e\perp}, u_{e\parallel},$
$u_{i\perp}, u_{i\parallel}$ } electron and ion velocity components, defined on p. 17

$\vec{u}_s, \vec{u}_c,$
$\vec{u}_{s+}, \vec{u}_{c+}$ } seed and carrier neutral and ion velocities

V   voltage

W   distance between electrodes

$\mathcal{W}_{th}$ thermodynamic work delivered by cycle

w, v   parameters in eq. (B7)

X_c, X_s degree of ionization of carrier and seed

x   axial coordinate

y $(p_L/p_H)^{(\gamma-1)/\gamma}$

Z   statistical weight

z T_2/T_4

α polarizability

β Hall parameter

γ ratio of specific heats

Δ	composite loss factor
δ_{ej}	loss factor for collision with j^{th} species
ϵ_{eff}	effective emissivity of radiator
ϵ_0	dielectric constant
η_{comp}	compressor efficiency
η_{conv}	conversion effectiveness
η_r	regenerator effectiveness
η_S	isentropic efficiency
η_{th}	thermal efficiency
Θ_e, Θ_i	parameters defined in eq. (34)
λ	relative thermal speed, eq. (27)
$\left.\begin{array}{l} \mu_{ec}, \mu_{es}, \\ \mu_{cc}, \mu_{cs}, \\ \mu_{ss}, \end{array}\right\}$	reduced mass
ν_{AB}	average collision frequency for momentum transfer from species A to B
$\tilde{\nu}_{ej}$	electron collision frequency for energy exchange with j^{th} species
$\left.\begin{array}{l} \nu_{ec}, \nu_{es}, \\ \nu_{ec^+}, \nu_{es^+}, \\ \nu_{c^+c}, \nu_{s^+c}, \\ \nu_{c^+s}, \nu_{s^+s}, \end{array}\right\}$	collision frequencies
ν_{en}, ν_{ei}	electron neutral collision frequency and electron ion collision frequency
ν_{in}	ion-neutral collision frequency
ξ	interacting length

34

Π	power output
ρ	density
Σ	nondimensional conductivity
σ	electrical conductivity
σ_{SB}	Stefan-Boltzman constant
Υ	parameter defined in eq. (12)
φ	potential
ψ	ion slip factor defined in eq. (43)
Ω_e, Ω_i	parameters defined in eq. (34)
ω	cyclotron frequency

Subscripts:

A,B	species
a	atom
c	carrier
coll	collision
comp	compressor
const	constant
e	electron
H	high
i	ion
L	low
max	maximum
n	neutral
rad	radiated
S	isentropic
s	seed

O   entrance condition

Superscripts:

$\rightarrow$ vector

$+$ ionized particle

$*$ moving coordinate

APPENDIX B

THERMODYNAMIC CYCLE EFFICIENCY

A Brayton cycle is considered with temperatures defined as shown in figure 9. The compressor efficiency, generator (isentropic) efficiency, and the regenerator effectiveness are defined as follows:
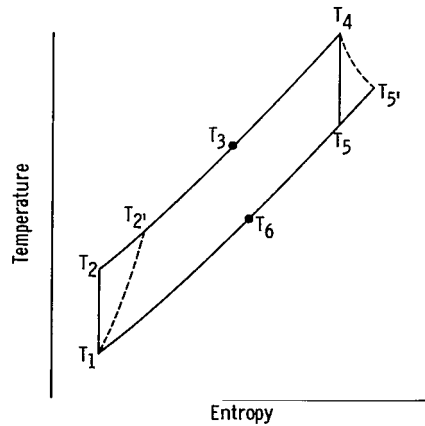
$$T_2 - T_1 = \eta_{comp}(T_{2'} - T_1)$$

$$\eta_S(T_4 - T_5) = T_4 - T_{5'} \tag{B1}$$

$$T_3 - T_{2'} = T_{5'} - T_6 = \eta_r(T_{5'} - T_{2'})$$

where the primed subscripts denote actual state points in figure 9. It is of interest to relate the generator efficiency η_S to the variables defined in the text and to discuss some of the implications of the concept. The effi-
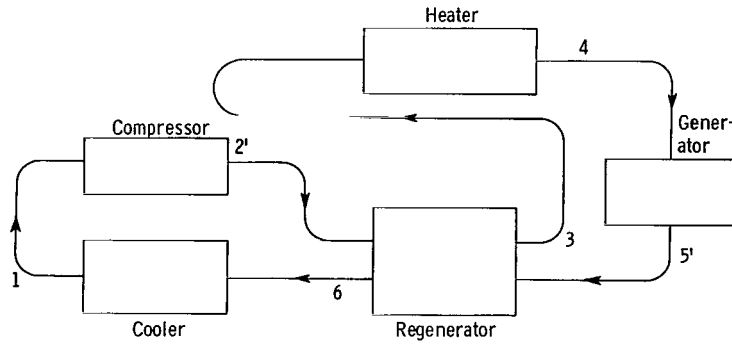
(a) Schematic.

(b) Temperature-entropy diagram.

Figure 9. - Brayton cycle temperature definitions.

ciency η_S can be expressed in terms of the solution to the generator equations as follows: From the definition of η_S:

$$\eta_S = \frac{T_4 - T_{5'}}{T_4 - T_5} = \frac{\eta_{conv}}{1 - \dfrac{T_5}{T_4}} = \frac{\eta_{conv}}{1 - y}$$

However, $y = (T_5/T_4) = (p_L/p_H)^{(\gamma-1)/\gamma}$ must also be expressed in terms of the generator variables. The ratio of total pressures p_L/p_H is expressed in terms of the dimensionless exit static pressure P, the exit gas velocity U, and the total temperature ratio $T_{5'}/T_4$:

$$\frac{p_L}{p_H} = \frac{P\gamma M_0^2}{\left(P\gamma M_0^2 U\right)^{\gamma/(\gamma-1)}} \left(\frac{T_{5'}}{T_4}\right)^{\gamma/(\gamma-1)}$$

so that

$$\eta_S = \frac{\eta_{conv}}{1 - \dfrac{1 - \eta_{conv}}{U(\gamma M_0^2 P)^{1/\gamma}}}$$

It should be noted that this isentropic efficiency is based on total properties. An isentropic change in total enthalpy that is not zero can occur if work is being done. This can be illustrated by an argument due to F. A. Lyman (of Lewis Research Center) as follows. From equation (3),

$$\rho u \frac{d}{dx}\left(h + \frac{u^2}{2}\right) = jE_{\perp}$$

Multiplying equation (2) by u and subtracting from equation (3) yield

$$u\rho\left(\frac{dh}{dx} - \frac{1}{\rho}\frac{dp}{dx}\right) = j(E_{\perp} + uB) = \frac{j^2}{\sigma}$$

From the Second Law of Thermodynamics, however, the left side of this equation can be written as

$$u\rho T \frac{ds}{dx} = \frac{j^2}{\sigma}$$

so that a constant entropy process can occur if σ approaches infinity. Hence, for a magnetohydrodynamics generator, the isentropic efficiency compares the actual generator to a generator using an infinitely conducting working fluid.

The parameters y and z are defined as

$$y = \left(\frac{p_L}{p_H}\right)^{(\gamma-1)/\gamma}$$

$$\left.\begin{array}{c} \\ \\ z = \dfrac{T_2}{T_4} \end{array}\right\} y, z \leq 1$$

The thermodynamic efficiency for zero pressure drop through the heater, regenerator, and cooler may be expressed in terms of these parameters as

$$\eta_{th} = \frac{(\eta_S \eta_{comp} - z)(1 - y)}{\eta_{comp} - \{z(1 - \eta_r)[1 - (1 - \eta_{comp})y] + \eta_r \eta_{comp}[1 - (1 - y)\eta_S]\}} \quad (B2)$$

If the cycle is to be used in the space environment, then it is desirable to minimize radiator area. The temperature ratio z, which minimizes the area, can now be determined. The heat radiated per unit electric power developed can be expressed as

$$\frac{Q_{rad}}{\mathcal{W}_{th}} = \frac{1 - \eta_{th}}{\eta_{th}}$$

where

$$Q_{rad} = \epsilon_{eff} \sigma_{SB} A_r T_{ave}^4$$

and

$$T_{ave}^4 = \frac{3T_6^3 T_1^3}{T_6^2 + T_6 T_1 + T_1^2} \quad (B3)$$

The area A_r required for a fixed maximum temperature T_4 can be obtained from

$$\frac{\epsilon_{eff} \sigma_{SB} T_4 A_r}{\mathcal{W}_{th}} = \frac{1 - \eta_{th}}{\eta_{th}} \left(\frac{T_4}{T_{ave}}\right)^4 \quad (B4)$$

where σ_{SB} is the Stefan-Boltzmann constant. Equation (B3) is rewritten in terms of

$$a = (1 - \eta_r)\left[1 - (1 - y)\eta_S\right]$$

$$b = \frac{\eta_r}{\eta_{comp}}\left[y\eta_{comp} + (1 - y)\right]$$
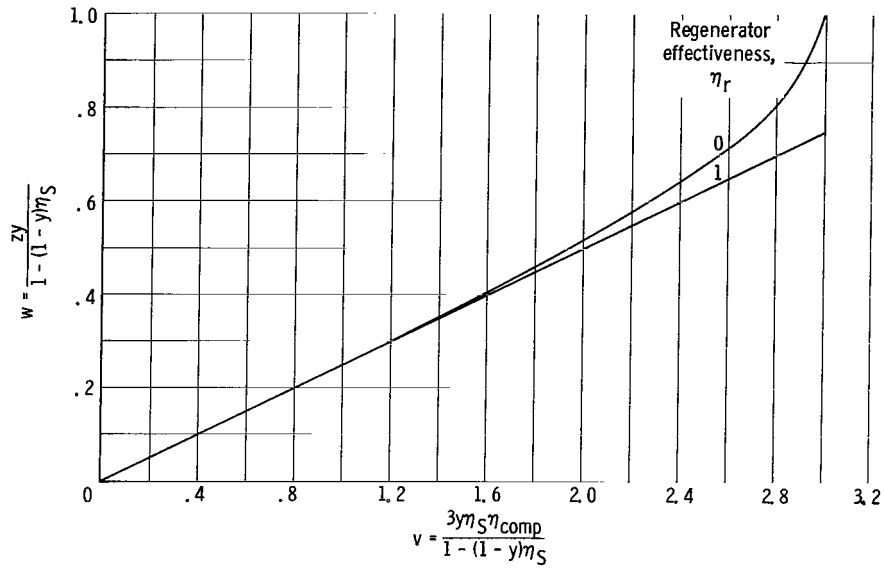
Figure 10. - Effect of regenerator effectiveness on solution of equation (B8).

by using equation (B3) to evaluate $(T_4/T_{ave})^4$ and (B1) to eliminate the temperature terms. Then the area per unit power output becomes

$$\frac{\epsilon_{eff} \sigma_{SB} T_4^4 A_r}{W_{th}} = \frac{1 - \eta_{th}}{3\eta_{th}} \frac{1}{a + (b - y)z} \left[\frac{1}{y^3 z^3} - \frac{1}{(a + bz)^3} \right] \qquad (B5)$$

Differentiation with respect to z produces the following equation for z, which minimizes A_r in equation (B3):

$$z \left[4 - \frac{ay^3 z^3}{(a + bz)^4 - by^3 z^4} \right] = 3\eta_S \eta_{comp} \qquad (B6)$$

The solution to this fifth-degree polynomial can be obtained in two special cases. The parameters w and v are defined as

$$\left. \begin{aligned} w &= \frac{yz}{1 - (1 - y)\eta_S} \\[2em] v &= \frac{3y\eta_S \eta_{comp}}{1 - (1 - y)\eta_S} \end{aligned} \right\} \qquad (B7)$$

40

Equation (B4) then becomes

$$w\left[4 - \frac{(1 - \eta_r)w^3}{\left(1 - \eta_r + \frac{b}{y} w\right)^4 - \frac{b}{y} w^4}\right] = v \tag{B8}$$

It may be seen that when $\eta_r = 1$

$$w = \frac{v}{4} \tag{B9}$$

and when $\eta_r = 0$ (and $b = 0$),

$$w(4 - w^3) = v \tag{B10}$$

These two solutions, which are plotted in figure 10, are nearly the same for $v \leq 2$. As a matter of fact, there is a condition for which the solutions will all be the same, namely, when the second term in the brackets of equation (B4) is small compared to 4. It can be shown that if

$$\eta_S \geq \eta_{conv} + \frac{1 - \eta_r - \eta_{conv}}{\eta_{comp}(1 + \eta_r)}$$

where

$$\eta_S(1 - y) = \eta_{conv}$$

then the second term will be less than 0.4. If $\eta_r = 1$, the inequality is always true. For the remainder of the analysis it will be assumed that the parameters are chosen such that this inequality is satisfied. Then, the value of z that minimizes A_r is

$$z = \frac{3}{4} \eta_S \eta_{comp}$$

and the thermodynamic cycle efficiency may be written as

$$\eta_{th} = \frac{\frac{1}{4} \eta_{conv}}{\eta_r \eta_{conv} + (1 - \eta_r)\left[1 - \frac{3}{4} \eta_{conv}\left(1 + \eta_{comp} \frac{y}{1 - y}\right)\right]} \tag{B11}$$

For the limiting values of U, η_{conv} in equation (11) becomes

41

$$\eta_{conv} = \frac{\gamma - 1}{M_1} (1 - K_{max})(K_{max} - M_1) \qquad K > K_\infty$$

or

$$\eta_{conv} = \frac{K_1(1 - U_{ch})(U_{ch} - M_1)}{(U_{ch} - K_1)M_1} \qquad K < K_\infty$$

APPENDIX C

DERIVATION OF ION-NEUTRAL CROSS SECTION AND COLLISION FREQUENCY

An encounter is considered between a singly charged ion and an atom of polarizability α. The polarizability is defined so that an electric field $\vec{E}_1$ will induce in the atom an electric dipole moment $\vec{g}$ satisfying[2]

$$\vec{g} = 4\pi\epsilon_0 \alpha \vec{E}_1 \tag{C1}$$

The atom is located at the origin, and the ion at $\vec{r}_1$. The electric field at the origin, due to the ion, is the field that gives rise to the atom's polarization; thus,

$$\vec{E}_1 = -\frac{e\hat{r}_1}{4\pi\epsilon_0 r_1^2} \tag{C2}$$

where $\hat{r}_1 = \vec{r}_1/r_1$. The dipole moment induced by the ion is then

$$\vec{g} = 4\pi\epsilon_0 \alpha \vec{E}_1 = -\frac{\alpha e}{r_1^2}\hat{r}_1 \tag{C3}$$

The dipole $\vec{g}$ gives rise to its own field $\vec{E}_2$ given generally by

$$\vec{E}_2 = \frac{1}{4\pi\epsilon_0 r^3}(3\hat{\hat{rr}} - \hat{\hat{I}}) \cdot \vec{g} \tag{C4}$$

where $\hat{\hat{I}}$ is the unit dyad.

In particular, for $\vec{r} = \vec{r}_1$ (i.e., at the ion),

$$\vec{E}_2 = -\frac{2\alpha e}{4\pi\epsilon_0 r_1^5}\hat{r}_1 \tag{C5}$$

The force $\vec{F}$ acting between the ion and the polarized atom is thus given by

$$\vec{F} = e\vec{E}_2 = -\frac{2\alpha e^2}{4\pi\epsilon_0 r_1^5}\hat{r}_1 \tag{C6}$$

---

[2]Nearly all data regarding polarizability have been compiled in cgs - esu units. In this system, α (in cu cm) is defined by $\vec{p} \equiv \alpha\vec{E}$, which becomes, in rationalized mks units, equation (C1) where $\alpha_{mks} = 10^6\alpha_{cgs}$.
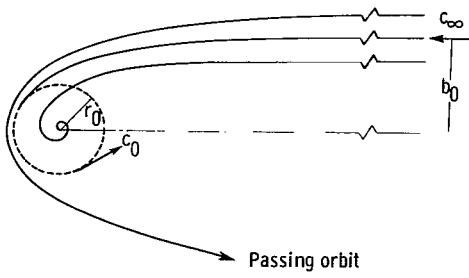
Figure 11. – Schematic of inward-spiraling and passing orbits.

and the potential φ, adjusted to be zero at $r_1 = \infty$, may be written as

$$\varphi = -\frac{\alpha e^2}{8\pi\epsilon_0 r^4} \qquad (C7)$$

by dropping the subscript on r. In order to ensure that the estimate for the ion-neutral collision cross section for momentum transfer is conservative (i.e., is an underestimate), the cross section is quite arbitrarily equated to πb_0^2, where b_0 is that impact parameter which separates inward-spiraling orbits from passing orbits (see fig. 11). To find the cross section three equations are employed: conservation of angular momentum, conservation of energy, and an asymptotic form of the momentum equation which states that the orbit approaches a circle, with the attractive polarization force balanced by the repulsive centrifugal force. These are, respectively,

$$\mu b_0 c_\infty = \mu r_0 c_0 \qquad (C8a)$$

$$\frac{1}{2}\mu c_\infty^2 = \frac{1}{2}\mu c_0^2 - \frac{\alpha e^2}{8\pi\epsilon_0 r_0^4} \qquad (C8b)$$

$$\frac{\mu c_0^2}{r_0} = \frac{\alpha e^2}{2\pi\epsilon_0 r_0^5} \qquad (C8c)$$

where μ is the reduced mass, c_∞ is the approach speed, and c_0 is the speed in the circular orbit of radius r_0. Eliminating c_0^2 between equations (C8b) and (C8c) yields

$$r_0^4 = \frac{\alpha e^2}{4\pi\epsilon_0\mu}\frac{1}{c_\infty^2} \qquad (C9)$$

while eliminating r_0 between equations (C8b) and (C8c) yields

$$c_0^2 = 2c_\infty^2$$

Using these relations together with equation (C8a) yields

$$\pi b_0^2 = \pi r_0^2\left(\frac{c_0}{c_\infty}\right)^2 = 2\pi r_0^2 = 2\pi\left(\frac{\alpha e^2}{4\pi\epsilon_0\mu}\right)^{1/2}\frac{1}{c_\infty} = \left(\frac{\pi\alpha e^2}{\epsilon_0\mu}\right)^{1/2}\frac{1}{c_\infty} \qquad (C10)$$

Thus, the conservative estimate for the collision cross section for momentum transfer between species A^+ and B (taking $m_{A^+} = m_A$) is

$$\mathscr{Q}_{A^+B} = \left(\frac{\pi\alpha_B e^2}{\epsilon_0 \mu_{AB}}\right)^{1/2} \frac{1}{c_{A^+B}} \tag{C11}$$

Abbreviating c_{A^+B} to c and defining $\alpha = \sqrt{2kT/\mu_{AB}}$ yield the average collision frequency, which is given by (see eq. (27))

$$\nu_{A^+B} = n_B \sqrt{\frac{8kT}{\pi\mu_{AB}}} \frac{4}{3} \frac{1}{\lambda^6} \int_0^\infty \mathscr{Q}_{A^+B}(c) c^5 e^{-c^2/\lambda^2} \, dc$$

$$= n_B \left(\frac{\pi\alpha_B e^2}{\epsilon_0 \mu_{AB}}\right)^{1/2} \frac{8}{3\sqrt{\pi}} \frac{1}{\lambda^5} \int_0^\infty c^4 e^{-c^2/\lambda^2} \, dc$$

$$= n_B \left(\frac{\pi\alpha_B e^2}{\epsilon_0 \mu_{AB}}\right)^{1/2} \tag{C12}$$

REFERENCES

1. Sutton, G. W.: The Theory of Magnetohydrodynamic Power Generators. Rep. R62SD990, General Electric Co., Dec. 1962, pp. 155-200.

2. Freedman, Steven I.: Thermodynamic Considerations for Magnetohydrodynamic Space Power Systems. Rep. R62SD83, General Electric Co., Sept. 1962.

3. Voshall, R. E., and Emmerich, W. S.: Small Rankine Cycle MHD Systems for Space Power. Proc. Fifth Symposium on Eng. Aspects of Magnetohydrodynamics, Inst. Elect. Eng., Apr. 1-2, 1964, pp. 65-67.

4. Elliot, David G.: Two-Fluid Magnetohydrodynamics Cycle for Nuclear-Electric Power Conversion. ARS Jour. vol. 32, no. 6, June 1962, pp. 924-928.

5. Sternglass, E. J., Tsu, T. C., Griffith, G. L., and Wright, J. H.: MHD Power Generation by Non-Thermal Ionization and Its Application to Nuclear Energy Conversion. Proc. Third Symposium on Eng. Aspects of Magnetohydrodynamics, Mar. 28-30, 1962.

6. Gourdine, M. C.: Non-Equilibrium R.F. Plasmas for Magnetogasdynamic Energy Conversion. Symposium on Magnetoplasmadynamic Electrical Power Generation, Inst. Elect. Eng. King's College, Univ. Durham, Newcastle Upon Tyne, Sept. 6-8, 1962.

7. Maitland, A.: A Criterion for Assessing Methods of Producing Nonequilibrium Ionization. Symposium on Magnetoplasmadynamic Electrical Power Generation, Inst. Elect. Eng., King's College, Univ. Durham, Newcastle Upon Tyne, Sept. 6-8, 1962.

8. Kerrebrock, Jack L.: Non-Equilibrium Effects on Conductivity and Electrode Heat Transfer in Ionized Gases. Tech. note 4, C.I.T., Nov. 1960.

9. Talaat, Mostafa: Magnetoplasmadynamic Electrical Power Generation with Nonequilibrium Ionization. Symposium on Magnetoplasmadynamic Electrical Power Generation, Inst. Elec. Eng., King's College, Univ. Durham, Newcastle Upon Tyne, Sept. 6-8, 1962.

10. Hurwitz, H., Jr., Sutton, G. W., and Tamor, S.: Electron Heating in Magnetohydrodynamic Power Generators. ARS Jour., vol. 32, no. 8, Aug. 1962, pp. 1237-1243.

11. Lyman, Frederic A., Goldstein, Arthur W., and Heighway, John E.: Effect of Seeding and Ion Slip on Electron Heating in a Magnetohydrodynamic Generator. NASA TN D-2118, 1964.

12. Harris, L. P., and Cobine, J. D.: The Significance of the Hall Effect for Three MHD Generator Configurations. Jour. of Eng. for Power (Trans. ASME), ser. A, vol. 83, Oct. 1961, pp. 392-396.

13. Neuringer, J. L.: Optimum Power Generation Using a Plasma as the Working Fluid. TN 59-571, Office Sci. Res., May 1959.

14. Coe, W. B., and Eisen, C. L.: The Performance Characteristics of a Constant Area MHD Energy Converter with Assumed Constant Plasma Conductivity. Rep. PPL-TN60-7, Republic Aviation Corp., Mar. 1, 1960.

15. Coe, W. B., and Eisen, C. L.: The Effect of Variable Plasma Conductivity on MHD Energy Converter Performance. Rep. PPL-TR-60-16(176), Republic Aviation Corp., Oct. 1960.

16. Way, S.: Magnetohydrodynamic Power Generation. Sci. Paper 6-40509-2-P2, Westinghouse Res. Lab., Apr. 1, 1960.

17. McNab, I. R., and Cooper, N. A.: Flow Processes in MPD Generators. Rep. IRD-63-82, Int. Res. Dev. Co., Ltd., Oct. 1963.

18. Pai, Shih-I: Magnetogasdynamics and Plasma dynamics. Springer Verlag (Berlin), 1962, p. 39.

19. Garrett, R. D., and Oates, G. C.: Channel Flow Solutions for a Crossed Field Accelerator. Tech. Memo. 3, Boeing Sci. Lab., Mar. 1963.

20. Ben Daniel, D. J., and Tamor, S.: Non-Equilibrium Ionization in Magnetohydrodynamic Generators. Rep. 62-RL-(2922-E), General Electric Co., Jan. 1962.

21. Burgers, J. M.: Selected Topics from the Theory of Gas Flow at High Temperatures. V. The Application of Transfer Equations to the Calculation of Diffusion, Heat Conduction, Viscosity, and Electric Conductivity. Tech. Notes BN-124a-b, pts. 1-2, Inst. for Fluid Dynamics and Appl. Math., Univ. of Md., May 1958.

22. Present, Richard David: Kinetic Theory of Gases. McGraw-Hill Book Co., Inc., 1958.

23. Brown, Sanborn: Basic Data of Plasma Physics. MIT Tech. Press (Cambridge), 1959, pp. 6; 7; 31.

24. Spitzer, Lyman, Jr.: Physics of Fully Ionized Gases. Second Ed., Intersci. Pub., 1962, p. 133.

25. Chanin, Lorne M., and Biondi, Manfred A.: Temperature Dependence of Ion Mobilities in Helium, Neon, and Argon. Phys. Rev., vol. 106, no. 3, May 1, 1957, pp. 473-479.

26. Lutz, Michael A.: Radiant Energy Loss from a Cesium-Argon Plasma to an Infinite Plane Parallel Enclosure. Rep. 175, Avco-Everett Res. Lab., Sept. 1963.

"The aeronautical and space activities of the United States shall be conducted so as to contribute . . . to the expansion of human knowledge of phenomena in the atmosphere and space. The Administration shall provide for the widest practicable and appropriate dissemination of information concerning its activities and the results thereof."

—NATIONAL AERONAUTICS AND SPACE ACT OF 1958

NASA SCIENTIFIC AND TECHNICAL PUBLICATIONS

TECHNICAL REPORTS: Scientific and technical information considered important, complete, and a lasting contribution to existing knowledge.

TECHNICAL NOTES: Information less broad in scope but nevertheless of importance as a contribution to existing knowledge.

TECHNICAL MEMORANDUMS: Information receiving limited distribution because of preliminary data, security classification, or other reasons.

CONTRACTOR REPORTS: Technical information generated in connection with a NASA contract or grant and released under NASA auspices.

TECHNICAL TRANSLATIONS: Information published in a foreign language considered to merit NASA distribution in English.

TECHNICAL REPRINTS: Information derived from NASA activities and initially published in the form of journal articles.

SPECIAL PUBLICATIONS: Information derived from or of value to NASA activities but not necessarily reporting the results ·of individual NASA-programmed scientific efforts. Publications include conference proceedings, monographs, data compilations, handbooks, sourcebooks, and special bibliographies.

Details on the availability of these publications may be obtained from:

SCIENTIFIC AND TECHNICAL INFORMATION DIVISION
NATIONAL AERONAUTICS AND SPACE ADMINISTRATION
Washington, D.C. 20546